UKRAINIAN JOURNAL OF MECHANICAL ENGINEERING AND MATERIALS SCIENCE
Vol. 3, No. 1, 2017

Bohdan Diveyev
Lviv Polytechnic National University, Lviv, Ukraine

DYNAMIC PROPERTIES PREDICTIONS FOR LAMINATED PLATES BY HIGH ORDER THEORIES

Received: February 7, 2017 / Revised: March 29, 2017 / Accepted: June 26, 2017

Abstract. The main aim of this study is to predict the elastic and damping properties of composite laminated plates. Some approximate methods for the stress state predictions for laminated plates are presented. For simple uniform bending and transverse loading conditions, this problem has an exact elasticity solution. This paper presents a new stress analysis method for the accurate determination of the detailed stress distributions in laminated plates subjected to cylindrical bending. The present method is adaptive and does not rely on strong assumptions about the model of the plate. The theoretical model described here incorporates deformations of each sheet of the lamina, which account for the effects of transverse shear deformation, transverse normal strain-stress and nonlinear variation of displacements with respect to the thickness coordinate. Dynamic and damping predictions of laminated plates for various geometrical, mechanical and fastening properties are defined. The comparison with the Timoshenko beam theory is systematically done for analytical and approximation variants.

The values of damping are got at a bend in three- and five-layered plates. For the three-layered plates the equivalent beam of Timoshenko exactly approximates a “sandwich” (with a soft damping kernel) dynamic properties of sandwich in a wide frequency range. For a plate with soft external layers the equivalent beam needs to be found in every frequency range separately. A hard bounded layer multiplies damping in a plate with soft external layers, however only at higher frequency of vibrations. For the high-frequency vibrations of plates the anomalous areas of diminishing of damping (for sandwiches) and increase are got for plates with soft covers. At the moderate amount of approximations the exact divisions of tensions are got in the layers of plates, thus the stresses continuity and surface terms are approximated exactly enough. Unlike the widespread theories of plates with the terms set a priori on surfaces (as a rule levels to the zero tensions) the offered equations allow to satisfy and complicated boundary conditions, instead of only free fastened plates. It allowed to explore the row of important examples for plates fastened in a hard holder and to explore influence of not only plates but also construction of holder on damping.

Keywords: composite materials, laminated plates, Timoshenko beam, stress distribution, damping.

Introduction

Noise and vibration are of concern with many mechanical systems including industrial machines, home appliances, surface vehicle transportation systems, aerospace systems, and building structures. Many such mechanical structural system components are comprised of beam and plate like elements. The vibration of beam and plate structural systems can be reduced by the use of passive damping, once the system parameters, such as dynamic stiffness of the plate or beam, have been identified. In some cases of forced vibration, the passive damping that can be provided is insufficient and the use of active damping has become attractive. Active damping is still mostly only used with high first cost items such as automobiles and aircraft, since it is still too expensive to use with low cost items such a household appliances.

Structures composed of laminated materials are among the most important systems used in modern engineering and, especially, in the automobile and aerospace industries. The rapid increase in the industrial

use of these structures has necessitated the development of new analytical and numerical tools that are suitable for the analysis and study of the mechanical behaviour of such structures. The determination of stiffness parameters for complex materials such as fiber-reinforced composites is much more complicated than for isotropic materials, since composites are anisotropic and non-homogeneous. Many different approaches have now been produced for the identification of the physical parameters which directly characterize structural behaviour.

Since the late 1950s, many papers have been published on the vibration of sandwich structures [1–4]. All of the models discussed so far are based on the following assumptions: a) the viscoelastic layer undergoes only shear deformation and hence the extensional energy of the core is neglected; b) the face sheets are elastic and isotropic and their contribution to the shear energy is neglected, and c) in the face-sheets, plane sections remain plane and normal to the deformed centre lines of the face-sheets. However, as the frequency increases, the results calculated from these models disagree strongly with measurements.

For modelling laminated composite plates, it is important to have an effective general theory for accurately evaluating the effects of transverse shear stresses on the plate performance. It has long been recognized that higher- order laminated plate theories may provide an effective solution tool for accurately predicting the deformation behaviour of composite laminates subjected to bending loads [5–9]. It is well known that higher-order theories, which account for transverse shear and transverse normal stresses, generally provide a reasonable compromise between accuracy and simplicity although they are usually associated with higher-order boundary conditions that are difficult to interpret in practical engineering applications. Simple theories for laminated plates are most often incapable of determining the three-dimensional (3-D) stress field in the laminates. Thus, the analysis of composite laminates may require the use of a laminate-independent theory or a 3-D elasticity theory. Exact 3-D solutions [10–13] have shown the fundamental role played by the continuity conditions for the displacements and the transverse stress components at the interfaces between two adjacent layers for making an accurate analysis of multilayered composite thick plates. Further, these elasticity solutions demonstrate that the transverse normal stress plays a predominant role in these analyses. However, accurate solutions based on 3-D elasticity theory are often intractable. But this classical refined theory has some limitations. For comparatively thick plates, it is not sufficiently precise. Other limitations of this theory are found with investigations not only with freely supported plates, but with also rigidly or elastically clamped ones. This is caused by the assumption in this theory of zero free surface stresses. For rigidly clamped plates, the exact 3-D solution near the clamped edges is not submerged.

The unification of formulation of schemes of calculations, which order of equalizations is unreserved, are offered in (the arbitrary number of approximations, which are examined on the thickness of plate) [14-16]. A review of refined theories of laminated composite plates has been presented at [17–19]. A review of vibration damping in sandwich composite structures has been presented in [20].

Nevertheless, this classical refined theory has some limitations. For the comparatively thick plates it is not sufficiently precisely [9]. Other limitation of this theory is by investigations not only freely supported plates, but also rigidly or elastically clamped. This is caused by postulation in this theory the zero free surfaces stresses. For the rigidly clamped plate the exact 3-d solution near the edge of clamp has the un- discreteness.

However, accurate solutions based on 3-D elasticity theory are often intractable. The limitation in the analysis which based on the displacement formulation has motivated some recent researches in which it has been used the theorem of mixed variation for the dynamic analysis of multilayered plates [21, 22].

Damping analysis of composite materials and structures has been presented at [23–35]. However, this classical refined theory has some limitations. Other limitations of this theory are found with investigations not only with freely supported plates, but with also rigidly or elastically clamped ones. This is caused by the assumption in this theory of zero free surface stresses. For rigidly clamped plates, the exact 3-D solution near the clamped edges is not submerged. In [36-40] of a stable identification algorithm allowing one to uniquely determine the elastic modules, including the transverse ones are elaborated.

This study aims to predict the elastic and damping properties of composite laminated plates. The present method for the modelling of laminated composite plates does not rely on strong assumptions about the model of the plate. In this paper, numerical evaluations obtained for vibrations in isotropic, orthotropic and composite laminated plates have been used to determine the displacement field for the efficient analysis of vibrations in laminated composite plates. A semi-analytical method has been developed to obtain the natural frequencies of vibration of simply-supported laminated composite cross-ply plates. The continuity of the transverse stresses as well as the displacements has been explicitly satisfied at the lamina interfaces in these models. Further, these models have been formulated by considering a local Cartesian coordinate system at the mid-surface of each individual layer. Six degrees of freedom: three displacement components, u, v and w (along the x, y and z axis directions, respectively) and three transverse stress components are expressed at the bottom as well as the top surface of each individual layer. The time dependent axial and transverse displacements along the x, y and z axis directions at any point can be expressed using power series expansions.

Certain aspects of the laminated elements parametric discretization

We will consider the discretization of the laminated thin-walled element A in some detail. The parameters of $l_1, l_2,..., l_{N_R}$ describe the geometrical form of A, the number and thickness of the layers, and the mechanical properties of the materials of the layers. Their amount is limited. For composite materials, it is often necessary to determine the mechanical properties from the structural properties of the materials. In such cases, some of the parameters of $l_1, l_2,..., l_{N_R}$ will be derived from a great number of primary parameters of $x_1, x_2,..., x_{N_P}$, which characterize the mechanical properties of the fibers, the structure of composition of the material and some features of the process of polymerization. It should be noted that the thin-walled element A properties not directly dependent on the aggregate of the parameters $l_1, l_2,..., l_{N_R}$, but only on a certain combination of these parameters. It is actually possible to consider only the optimization of the parameters $s_1, s_2,..., s_{N_C}$ which depend on $l_1, l_2,..., l_{N_R}$. If we consider the set accordingly:

$$x_i \in \Xi, \quad l_i \in \Lambda, \quad s_i \in \mathrm{Z},$$

then the surjective reflections (when one element l_i of Λ corresponds a few (elements $x_1, x_2,..., x_{N_P}$ of Ξ and every element l_i has a prototype) of Ω_A, Ω_B will take place

$$\Xi \xrightarrow[\Omega_A]{} \Lambda \xrightarrow[\Omega_B]{} \mathrm{Z}.$$

The actual calculation and consequently the optimization will be conducted in the set of Z, which is far narrower than Λ, and even narrower than Ξ. Numerical schemes (*NS*) using hypotheses for the entire package of the laminated elements will especially demonstrate this narrowing. The scheme for the condensed modelling of the sandwich element wit the honeycomb core is presented in Fig. 1.

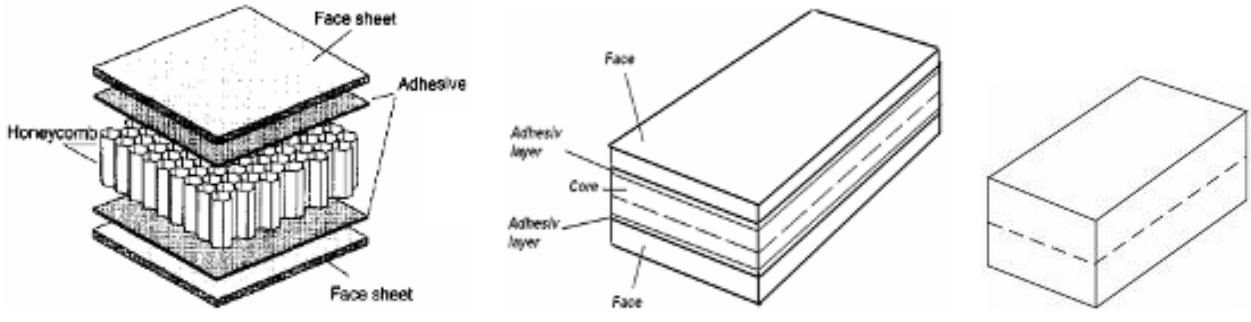

a *b* *c*

Fig. 1. *Heterogeneous 3-D model (a); heterogeneous 2-D model (b); homogeneous 2-D model (c)*

Detailed description of various types of sandwich panel theories may be found in [1–40]. A historical review of the available zigzag theories for elastic laminated plates and shells has been presented in [17–19].

Analytical modelling of the cylindrical bending of laminated plates

Exact solutions may be obtained in only a few cases for the deformations of laminated plates. These exact solutions exist in the case of static cylindrical bending of composite laminas.

3.1. Cylindrical bending of laminated plates subjected to loading by a moment.

The governing equations for the stresses are (the axis x is oriented along the middle line of the plate and the axis z is oriented normal to it).

$$\frac{\partial s_{xx}}{\partial x}+\frac{\partial t_{xz}}{\partial z}=0, \qquad \frac{\partial t_{xz}}{\partial x}+\frac{\partial s_{zz}}{\partial z}=0. \tag{1}$$

The solutions which express Hooke's law with respect to the stress components have the form

$$s_{xx}=C_{xx}e_{xx}+C_{xz}e_{zz}, \quad s_{zz}=C_{zx}e_{xx}+C_{zz}e_{zz}, \quad t_{xz}=Gg_{xz}. \tag{2}$$

For pure bending, the stress-strain state is uniform, thus

$$\frac{\partial t_{xz}}{\partial z}=-\frac{\partial s_{xx}}{\partial x}=0 \quad and \quad t_{xz}=0, \tag{3}$$

$$\frac{\partial s_{zz}}{\partial z}=-\frac{\partial t_{xz}}{\partial x}=0 \quad and \quad s_{zz}=0. \tag{4}$$

If the stress s_{xx} is not equal to zero, the following assumption must be made

$$s_{xx}=S(z). \tag{5}$$

The expressions for the displacements and the stress are obtained from Eqs. (1)-(5). The result is as follows.

$$\begin{gathered} u=xz, \; w=-0.5(a\,z^2+x^2), \\ s_{xx}=z\left(C_{xx}-a\,C_{xz}\right), \end{gathered} \tag{6}$$

where $a=C_{xz}/C_{zz}$.

For the bending moment we obtain

$$M=\int_{-H_p}^{H_p} z^2\left(C_{xx}-a\,C_{xz}\right)dz, \tag{7}$$

where H_p is one-half of the thickness of a lamina.

Since the materials may be non-homogeneous, $C_{xx}(z), a(z), C_{xz}(z)$ may all be functions of z. For a uniform Timoshenko beam of the same thickness, an equation for the bending rigidity of a uniform equivalent beam may be written with regard to the condition $\frac{dg}{dx}=1$.

$$E_T I=M\left(\frac{dg}{dx}\right)^{-1}=\int_{-H_p}^{H_p} z^2\left(C_{xx}-a\,C_{xz}\right)dz. \tag{8}$$

3.2. Cylindrical bending of laminated plates subjected to loading by a force.

In this case the primary assumptions are

$$s_{xx}=xS(z), \qquad t_{xz}=T(z). \tag{9}$$

The following expressions are obtained from Hooke's law

$$\begin{gathered} e_{xx}=\frac{\partial u}{\partial x}=xS^*, \; e_{zz}=\frac{\partial w}{\partial z}=-a_1xS^*, \\ S^*=\frac{S(z)}{1-a_1a_2}, \quad a_1=\frac{C_{xz}(z)}{C_{xx}(z)}, \quad a_2=\frac{C_{xz}(z)}{C_{zz}(z)}. \end{gathered} \tag{10}$$

Next, by integrating Eq. (10) for the displacement we obtain

$$u = \frac{x^2}{2} S^* + f(z), \quad w = -x \int_0^z a_1 S^* dz + y(x). \tag{11}$$

By substituting Eq. (11) into Eq. (1), we can derive the following equation for a symmetrically laminated plate. It also holds for plates with arbitrary laminations

$$u = \frac{c_1 x^2 z}{2C_{xx}} + c_1 \int_0^z \left(\int_0^z \frac{a_2 z}{C_{xx}} dz + \frac{t_{xz}}{G} \right) dz - c_2 z, \quad w = -\frac{c_1 x^3}{6C_{xx}} - c_1 x \int_0^z \frac{a_2 z}{C_{xx}} dz + c_2 x, \tag{12}$$

where for the tangential stress t_{xz} and the constant c_2 we have

$$t_{xz} = -c_1 \int_z^H (1 - a_1 a_2) z dz, \quad c_2 = \frac{c_1}{H_p} \int_0^{H_p} dz \left(\int_0^z \frac{a_2 z}{C_{xx}} dz + \frac{t_{xz}}{G} \right) dz. \tag{13}$$

In the above equations, c_1 is an arbitrary constant. If the tangential force Q is equated to unity, then the following equation may be obtained from Eqs. (12) and (13)

$$Q = \int_{-H_p}^{H_p} t_{xz} dz = 1 \Rightarrow c_1 = \left(\int_{-H_p}^{H_p} \left(\int_z^{H_p} (1 - a_1 a_2) z dz \right) dz \right)^{-1}. \tag{14}$$

Thus, by comparison with a uniform Timoshenko beam of the same cross section, we may write an equation for the transverse rigidity of a uniform equivalent beam

$$\frac{1}{2H_p G_T} = -c_1 \int_0^z \frac{a_2 z}{C_{xx}} dz + c_2 = -c_1 \int_0^z \frac{a_2 z}{C_{xx}} dz + \frac{c_1}{H_p} \int_0^{H_p} dz \left(\int_0^z \frac{a_2 z}{C_{xx}} dz + \frac{t_{xz}}{G} \right) dz. \tag{15}$$

Here the value t_{xz} is given by Eq. (13); G_T and E_T denote the Timoshenko beam moduli. It may be seen that the same bending rigidity is obtained from Eq. (12) as in Eq. (8).

Higher order asymptotic approach

Various high-order displacement models have been developed in the literature by considering combinations of displacement fields for in-plane and transverse displacements inside a mathematical sub-layer. In order to obtain more accurate results for the local responses, another class of laminate theories, commonly named as the layer-wise theories, approximate the kinematics of individual layers rather than a total laminate using the 2-D theories. These models have been used to investigate the phenomena of wave propagation as well as vibrations in laminated composite plates. Numerical evaluations obtained for wave propagation and vibrations in isotropic, orthotropic and composite laminated plates have been used to determine the efficient displacement field for economic analysis of wave propagation and vibration. The numerical method developed in this paper follows a semi-analytical approach with an analytical field applied in the longitudinal direction and a layer-wise power series displacement field employed in the transverse direction. The goal of the present paper is to develop a simple numerical technique, which can produce very accurate results compared with the available analytical solution. The goal is also to provide one with the ability to decide upon the level of refinement in higher order theory that is needed for accurate and efficient analysis.

Let us consider now such kinematic assumptions $(U = U_e - U_d)$ for a symmetrical three-layered plate of thickness $2H_p$ (only cylindrical bending is considered):

$$U_e - \begin{cases} u = \sum_{i,k} u_{ik}{}^e z^{2i-1} f_k(x), & 0 < z < H, \\ w = \sum_{i,k} w_{ik}{}^e z^{2i-2} g_k(x), & 0 < x < L, \end{cases} \tag{16}$$

$$U_d - \begin{cases} u = \sum_{i,k} u_{ik}{}^d (z-H)^i f_k(x), & H < z < H_p, \\ w = \sum_{i,k} w_{ik}{}^d (z-H)^i g_k(x) & 0 < x < L. \end{cases} \tag{17}$$

Here $f_k(x)$, $g_k(x)$ – are a priory known coordinate functions (for every beam clamp conditions), $u_{ik}{}^e$, $w_{ik}{}^e$, $u_{ik}{}^e$, $w_{ik}{}^e$ – unknown set of parameters.

By substituting Eqs. (16) by (2) into the Hamilton-Ostrogradsky variation equation

$$\int_{t_1}^{t_2}\int_V (s_{xx}de_{xx} + s_{zz}de_{zz} + t_{xz}de_{xz} - r\frac{\partial u}{\partial t}d\frac{\partial u}{\partial t} - r\frac{\partial w}{\partial t}d\frac{\partial w}{\partial t})dVdt = \int_{t_1}^{t_2}\int_S PdU\,, \tag{18}$$

and also assuming single frequency vibration ($u_{ik}^e = \bar{u}_{ik}^e e^{iwt}$, $w_{ik}^e = \bar{w}_{ik}^e e^{iwt}$, $u_{ik}^d = \bar{u}_{ik}^d e^{iwt}$, $w_{ik}^d = \bar{w}_{ik}^d e^{iwt}$) we obtain the set of linear algebraic equations for the amplitudes (matrixes A_i are given in Appendix A)

$$[A]\bar{U} = \begin{bmatrix} A_1 & A_d \\ A_d^T & A_2 \end{bmatrix}\begin{bmatrix} \bar{U}_e \\ \bar{U}_d \end{bmatrix} = f\,. \tag{19}$$

For a greater number of lamina this equation has the following form for each additional layer

$$U_d^n - \begin{cases} u = \sum_{i,k} u_{ik}\left(z - H^{(n)}\right)^i f_k(x), & H_n < z < H_P, \\ & 0 < x < L, \\ w = \sum_{i,k} w_{ik}{}^n\left(z - H^{(n)}\right)^i g_k(x), & n = 1, ..., N, \end{cases} \tag{20}$$

Here H_n are the low bounds of the n-*th* layer, respectively. Matrix $[A]$ is found by double integration through the thickness and along the length of the beam (see Appendix A, B). Note that, $N = 1$ and $N = 2$ represent the cases of symmetrical three- and five-layered plates, respectively.

The corresponding frequency equation for the material with the viscous damping should be written such

$$-w^2[M]\bar{U} + iw[C]\bar{U} + [K]\bar{U} = [A]\bar{U} = \bar{f}\,. \tag{21}$$

This is the traditional frequency domain method which is normally used in linear elastic system investigations. By taken into account first terms in (16) we obtain the kinematic assumptions of Timoshenko beam.

Numerical example – three-layered symmetrical beam (sandwich)

Let us consider a three-layered symmetrical beam. (See Fig. 2.) Its mechanical properties are chosen to be: core material (honeycomb polymer filled structure): the compressive modulus is 1.076 GPa; tensile modulus is 3.96 GPa; flexural modulus – 1.020 GPa; and shear modulus is 0.638 GPa. Face material (fibre composite material): tensile modulus is 26 GPa; flexural modulus ≈ 6 GPa; and shear modulus ≈ 0.6 GPa. These properties are concerned with the sandwich beam with the honeycomb filled core. Face fiber polymer material are rigid and the core is very soft in the tangential direction. In the calculations, the arithmetic mean value of the compressive modulus and the tensile modulus was chosen.

The values of the elastic constants E_T, G_T of an equivalent Timoshenko beam are presented in Fig. 3b. For the identification of the elastic modulus, a procedure was used which compares the elastic energy of the two beams: one of them – non-uniform, and other – uniform. The iso-lines given in Fig. 3 represent constant values of the difference between the Timoshenko beam elastic energy and the energy of an analytically modeled beam $\int_V (s_{xx}de_{xx} + s_{zz}de_{zz} + t_{xz}de_{xz})dV$. Two methods were applied: (a) analytical Eqs. (1)–(15), and (b) approximate Eqs. (16)–(21). Fig. 3 presents the theoretically derived

elasticity constants E_T, G_T (corresponding to the minimum difference in the energies) for the Timoshenko beam analogue of the sample beam described above. The small difference in the values is caused by the different elastic energy components, which are taken into account in the two cases. In the approximate method the transverse energy component $\int_V (s_{zz} de_{zz}) dV$) is very small and is not taken into account. For a symmetrical structure with identical face layers, the equivalent rigidity may be found from the Timoshenko beam theory by the use of Eqs. (8) and (15).

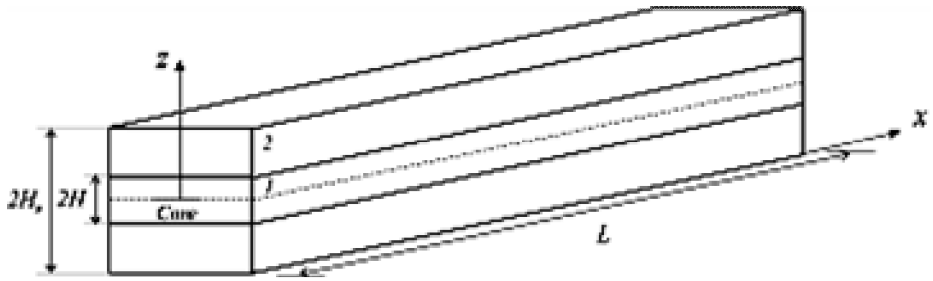

Fig. 2. *The sandwich beam with inner viscoelastic layer (1) (core) and identical face layers (2)*

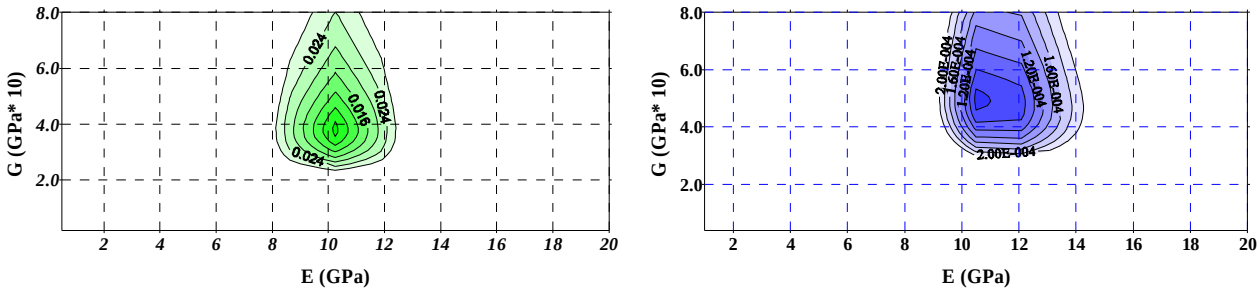

a *b*

Fig. 3. *Equivalent moduli E_T and G_T : a – analytical approach; b – approximate approach*

All of these properties are found in the first eigen-frequency region. But it is well known that the rigidity and damping properties of composite plates are frequency dependent. This phenomenon may be caused by a frequency dependent visco-elastic modulus or by a frequency dependent stress distribution through the plate thickness. The second case will be considered now.

Eigen-frequency of a uniform beam

Clamped-free beam. Dynamic properties of clamped-free beam are identical to centrally clamped symmetrical beam of the double length. A range of numerical experiments must be made to ensure that this theoretical approach is correct. Let us compare the eigen-frequencies of a clamped-free uniform isotropic beam for the following geometrical parameters: length L was chosen to be 0.3 m, thickness was chosen to be $H = 0.0130$ m. The elastic moduli were assumed to be as follows: $C_{xx} = C_{zz} = 240$ MPa, $G = 120$ MPa, and $C_{xz} = 103$ MPa (n = 0.3). The eigen-frequencies were obtained by means of FEM and Eqs. (21) by the cinematic assumption ($f_k(x) = g_k(x) = \sin(kp\,x/2L)$) for clamped-free beam (see Tables 1–4). The elements of system matrixes in (21) are calculated as in Appendixes A and B.

In the Table 1, in the first row, the mesh of the FEM grid in the *X*, *Z* plane is presented. In the last column, the mesh in the *Y* direction was doubled (N_y = 20). In Tables 2-4, the first row presents the number of approximations in the *X* and *Z* directions (see Eq. (16)). The modes of vibration are presented in Fig. 4.

In Tables 1–4 the rate of convergence of two methods and the agreement between the results may be seen (see the last column in Tables 1 and 4).

Beam simply supported at the ends. Let us consider simply supported at the ends beam. The modes of vibration for 3d-beam obtained by FEM are presented in Fig. 5. Length L was chosen to be 0.58 m, thickness was chosen to be $H = 0.0116$ m. The elastic moduli were assumed to be as follows: $C_{xx} = C_{zz} = 230$ MPa, $G = 90$ MPa, and n = 0.3.

Table 1

Eigen-frequencies of a clamped-free uniform isotropic beam obtained by means of FEM

N_f	(N_x×N_z) 60×9	150×9	300×9	600×9	600×9 (2)
1	20.5	19.9	19.7	19.6	19.2
2	128.3	124.3	123.2	122.9	120.4
3	356.7	345.4	342.3	341.4	335.4
4	690.0	667.7	661.6	659.9	649.8
5	1121.1	1083.7	1073.6	1070.9	1056.4
6	1641.0	1584.0	1568.8	1564.7	1546.1
7	2240.8	2159.3	2137.7	2131.9	2109.5
8	2954.5	2800.6	2771.2	2763.4	2737.5

Table 2

Eigen-frequencies of a clamped-free uniform isotropic beam obtained by means of Eqs. (22), $N_z = 1$

N_f	$N_x = 17$, $N_z = 1$	$N_x = 23$, $N_z = 1$	$N_x = 27$, $N_z = 1$	$N_x = 29$, $N_z = 1$	$N_x = 31$, $N_z = 1$
1	21.8	21.5	21.5	21.4	21.4
2	135.6	134.2	133.8	133.4	133.4
3	375.7	371.5	370.3	369.7	369.7
4	725.7	717.4	715.8	714.1	714.1
5	1178.7	1165.0	1161.8	1159.7	1158.7
6	1728.4	1702.9	1699.0	1697.8	1696.5
7	2363.6	2327.7	2318.8	2315.8	2312.8
8	3084.4	3024.6	3011.0	3006.0	3002.6

Table 3

Eigen-frequencies of a clamped-free uniform isotropic beam obtained by means of Eqs. (22), $N_z = 2$

N_f	$N_x = 17$, $N_z = 2$	$N_x = 23$, $N_z = 2$	$N_x = 27$, $N_z = 2$	$N_x = 29$, $N_z = 2$	$N_x = 31$, $N_z = 2$
1	19.8	19.5	19.5	19.4	19.4
2	122.7	121.7	121.3	121.0	121.0
3	340.7	337.3	336.1	335.6	335.6
4	659.1	652.0	650.5	648.9	648.9
5	1073.1	1061.0	1057.0	1055.0	1053.9
6	1574.1	1554.6	1548.5	1546.1	1543.6
7	2158.1	2126.6	2115.2	2112.4	2109.5
8	2819.2	2760.5	2750.8	2745.9	2742.7

Table 4

Eigen-frequencies of a clamped-free uniform isotropic beam obtained by means of Eqs. (22), $N_z = 3$

N_f	$N_x = 17$, $N_z = 3$	$N_x = 23$, $N_z = 3$	$N_x = 27$, $N_z = 3$	$N_x = 29$, $N_z = 3$	$N_x = 31$, $N_z = 3$
1	19.9	19.5	19.5	19.5	19.4
2	124.0	121.7	121.3	121.0	121.0
3	343.5	337.3	336.1	336.1	335.6
4	671.1	652.8	650.5	649.7	648.1
5	1066.0	1061.0	1057.0	1056.0	1053.9
6	1563.1	1554.6	1547.3	1544.8	1543.6
7	2153.8	2123.8	2115.2	2112.4	2109.5
8	2816.0	2763.8	2750.8	2745.9	2742.7

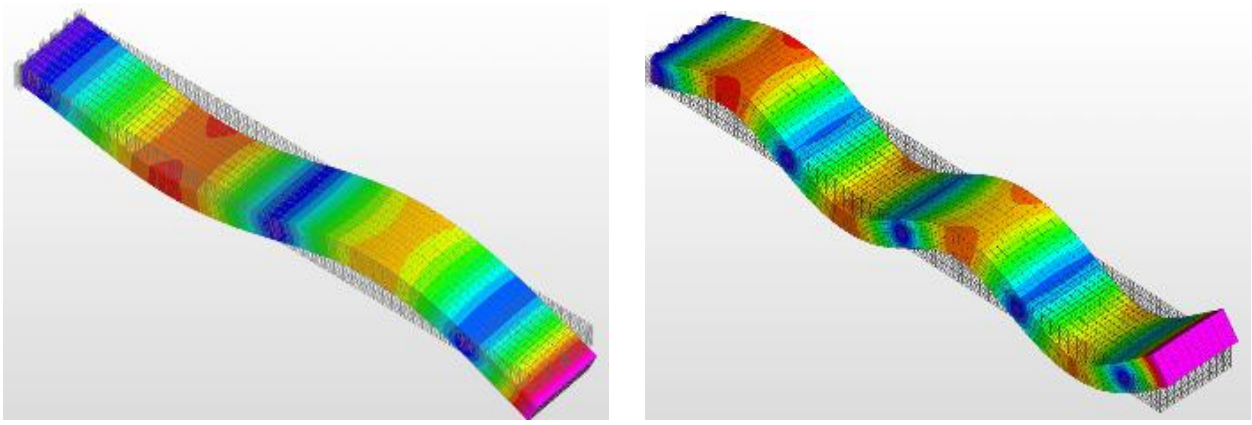

a *b*

Fig. 4. *Modes of beam vibration: a – the third mode, b – the sixth mode*

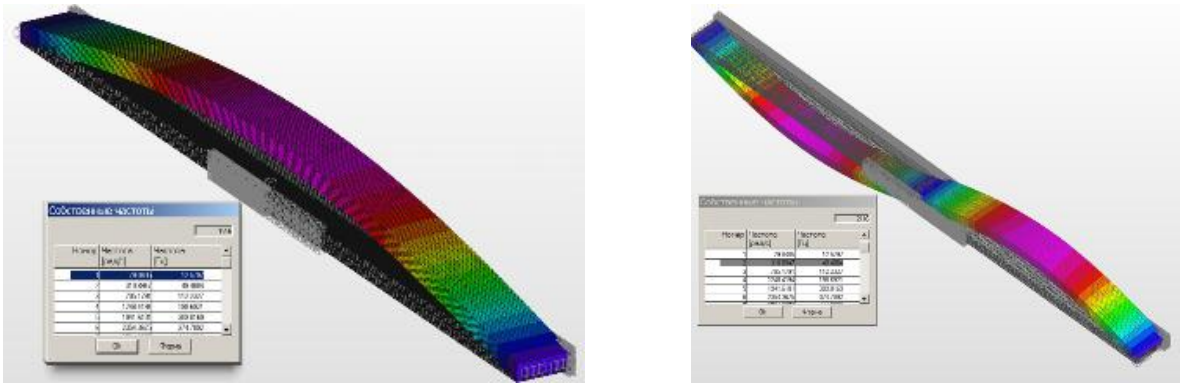

a *b*

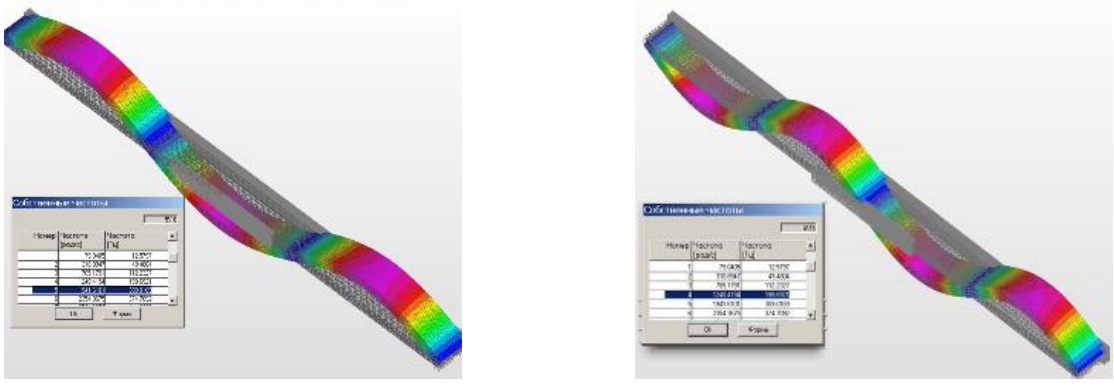

c *d*

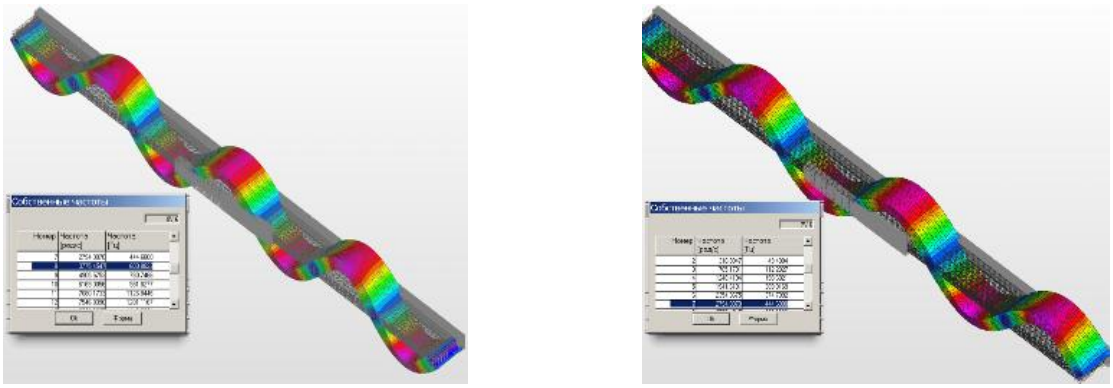

e *f*

Fig. 5. *Modes of beam vibration: a, c, e – symmetrical, b, d, f – asymmetrical modes*

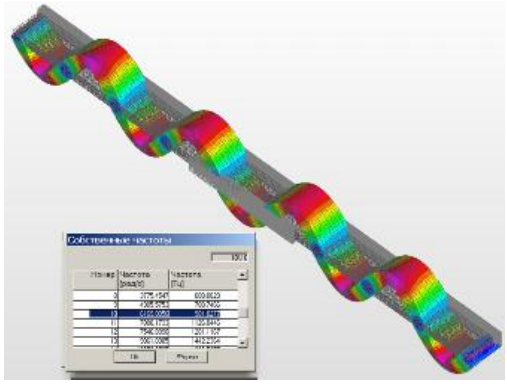

g

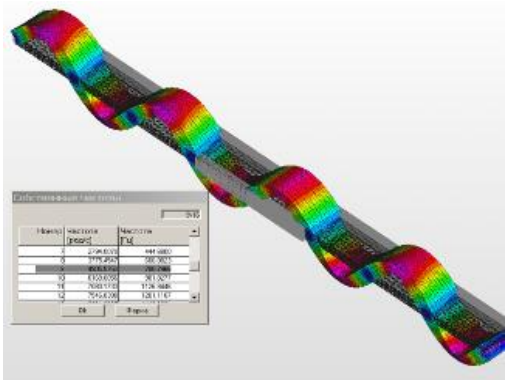

h

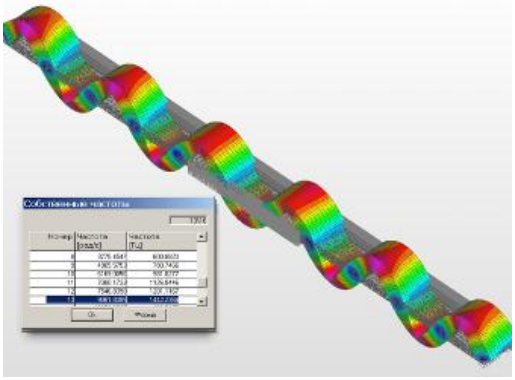

k

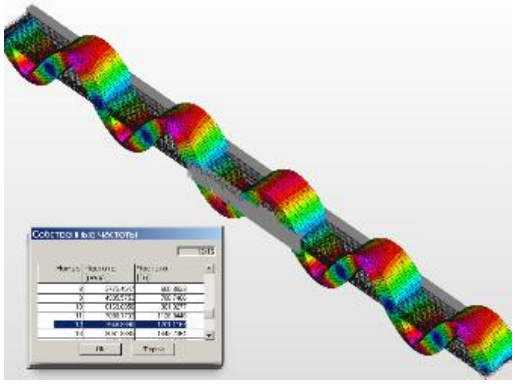

l

Continuation of fig. 5. *Modes of beam vibration: g, k – symmetrical; h, l – asymmetrical modes*

The modes of vibration for 2d-beam obtained by FEM are presented in Fig. 6.

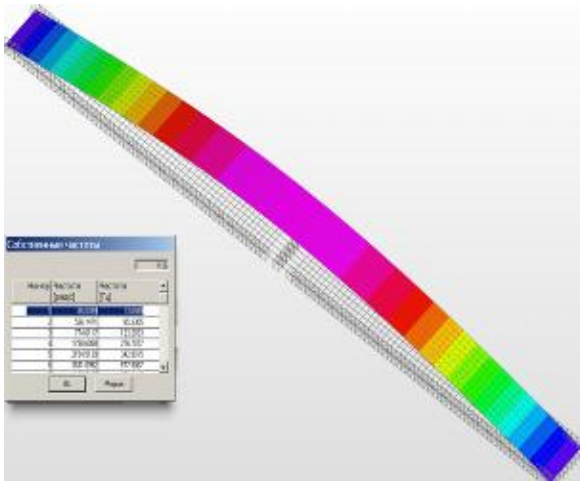

k

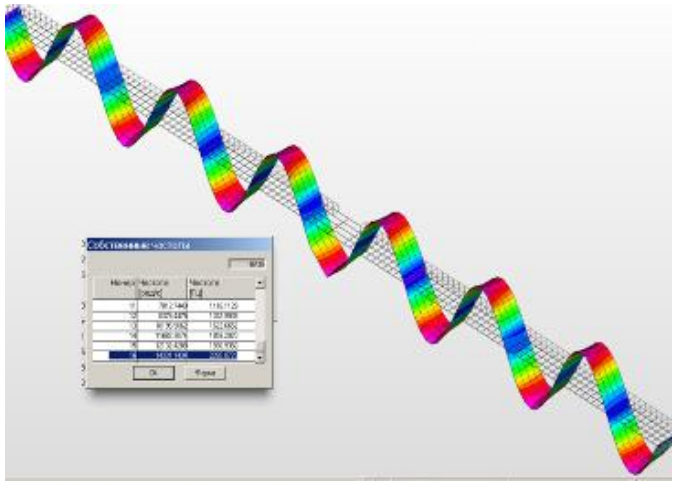

l

Fig. 6. *Symmetrical modes of beam vibration: a – the first mode; b – mode twelve*

The eigen-frequencies obtained by means of Eqs. (21) by $f_k(x)=\sin\left((2k-1)p\,x/2L\right)$ $g_k(x)=\cos\left((2k-1)p\,x/2L\right)$ in (20) and FEM are presented in Table 5.

As expected, the 3-d FEM dates are more exact and near to a precise analytical solution. For the 1-layer approximation the deviations for one layer theory are grater than for three layer theory. For the uniform beam result obtained by various beam theories are identical for $N_Z \geq 2$. The layers in the uniform beam are chosen arbitrarily. The numerical results are practically identical for an arbitrary layers thickness.

Table 5

Eigen-frequencies of a simply supported uniform isotropic beam obtained by means of FEM and analytical approximations

FEM		One layer theory		Three layer theory		
2-d beam	3-d beam	$N_Z=1$	$N_Z=2$	$N_Z=1$	$N_Z=2$	$N_Z=3$
13.13	12.56	13.30	12.22	12.22	12.22	12.22
118.43	112.16	116.49	110.01	110.01	110.01	110.01
330.32	308.88	316.80	306.05	306.05	306.05	306.05
650.82	600.46	622.96	592.91	600.35	592.91	592.91
1082.18	981.29	1021.92	983.32	992.90	983.32	983.32
1626.45	1441.97	1519.14	1460.33	1472.00	1460.33	1460.33
2285.87	1974.18	2114.61	2017.65	2045.12	2017.65	2017.65
3060.29	2569.30	2792.21	2664.88	2696.43	2664.88	2664.88
3952.38	3220.46	3545.67	3401.99	3419.79	3401.99	3401.99
4962.48	–	5300.08	4209.22	4248.85	4209.22	4209.22
6092.56	–	6272.83	5080.55	5124.09	5080.55	5080.55
–	–	7327.49	6033.80	6081.23	6033.80	6033.80
–	–	8436.04	7043.35	7094.60	7043.35	7043.35
–	–	9592.79	8103.51	8158.47	8103.51	8103.51

The eigen-frequencies obtained by means of Eqs. (21) by $f_k(x)=g_k(x)=\sin(kp\,x/2L)$ (clamped-free beam) in (20) and FEM are presented in Tables 6 as for one-layer theory so for layered theory.

Table 6

Eigen-frequencies of a clamped-free beam, analytical approximations

One layer theory				Three layer theory		
$N_Z=1$	$N_Z=2$	$N_Z=3$	$N_Z=4$	$N_Z=1$	$N_Z=2$	$N_Z=3$
23.28	22.91	22.91	22.91	22.91	23.04	23.04
135.81	133.00	133.00	130.32	30.32	131.87	131.87
740.39	703.30	684.78	684.78	678.66	677.58	677.58
1438.47	1322.40	1288.52	1280.12	1271.75	1265.23	1265.23
2098.96	1934.63	1873.25	1863.12	1842.93	1844.18	1844.18
2776.33	2531.60	2461.31	2438.10	2415.00	2411.21	2411.21
3428.85	3129.56	3025.50	2999.76	2974.13	2968.48	2968.48
4072.38	3733.34	3605.51	3563.39	3535.45	3521.59	3521.59
4715.51	4328.43	4175.53	4130.20	4100.12	4077.49	4077.49
5346.46	4934.52	4738.83	4690.53	4658.47	4638.61	4638.61
6017.01	6136.55	5864.11	5252.45	5218.52	5191.45	5191.45
6628.00	6757.72	6452.81	5810.36	5774.66	5739.73	5739.73
7268.54	7368.52	7010.65	6358.97	6340.28	6296.55	6296.55
7902.61	7984.78	7591.61	6932.33	6893.33	6846.65	6846.65

It is necessary to note that in practice the refined theory produces asymptotic estimated values for the natural frequencies when the degree of approximation in the thickness direction $N_z \geq 2$ for layer-wise theory. One-layer theory overestimates the eigen-frequencies for lower degree of approximation in the thickness direction.

Let us consider now the vibration testing of an anisotropic beam having the following geometrical parameters: length L varied from 0.6 m to 0.2 m and thickness $H=0.0127$ m. The elastic moduli are assumed to be as follows: $C_{xx}=C_{zz}=250$ MPa, $G=58$ MPa, and $C_{xz}=40$ MPa (foam material). The frequency response functions (FRF) for these beams are presented in Fig. 7 (Eqs. (16)–(21) were used). These functions were obtained for various ranges of approximations for various frequency domains (various beam lengths).

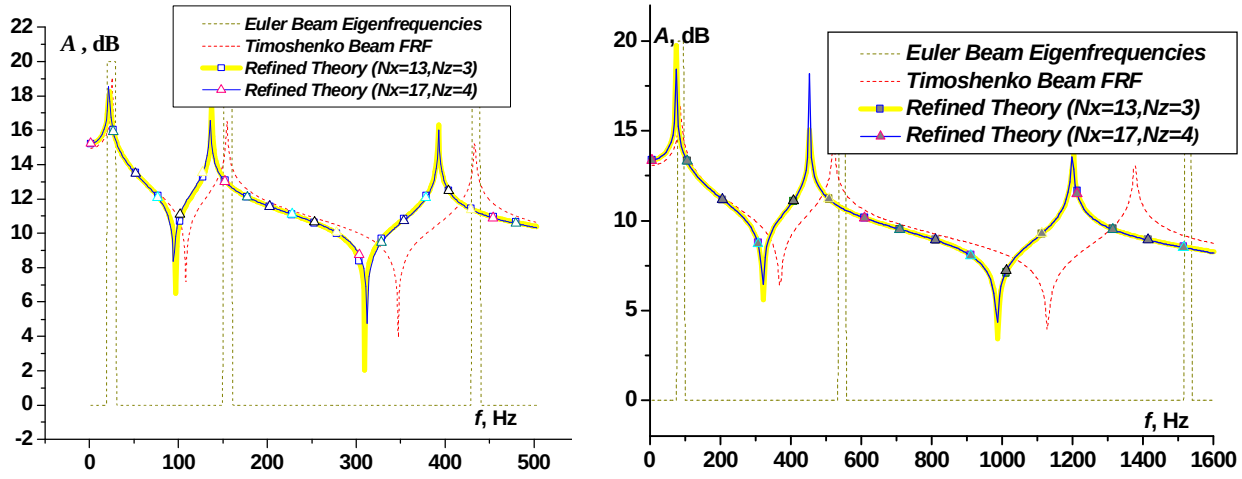

a *b*

Fig. 7. *FRF dependence for:*
a – beam with length $L = 0.6$ *m ; b – beam with length* $L = 0.2$ *m*

From the results obtained, it follows that the Euler beam theory overestimates the natural frequency values. It can be observed that the Timoshenko beam theory also overestimates the natural frequency values but less so than the Euler theory. Note that in practice the refined theory produces asymptotic estimated values for the natural frequencies when the degree of approximation in the longitudinal direction $N_x > 13$ and in the thickness direction $N_z \geq 2$.

Influence of anisotropy of elastic properties of the beam on its FRF

Let us investigate the effect of anisotropy of elastic properties of the beam on its amplitude-frequency response function. First, we will consider a homogeneous beam with the values of elastic constants given earlier; those values were assumed as initial, but the other parameters were varied. Fig. 8 shows the FRFs of beams with different elastic constants. The FRFs were calculated for a clamped-free beam, with excitation at its central clamped point. As seen from the Fig. 8, the effect of the elastic moduli C_{XX} and G on the FRF is marked over the entire range of frequencies, while the effect of the modulus C_{ZZ} and $C_{XZ} = n C_{XX}$ is observed only at the highest frequencies.

Next, we will consider a symmetric three-layer beam and examine the influence of anisotropy of layer materials on the FRF. The outer layers of the beam are rigid and have the following characteristics: h = $H2$ = =0.0005 m, C_{XX} = 17 GPa, C_{ZZ} =1.5 GPa, G = 580 MPa, and C_{XZ} = 700 MPa. The inner layer of thickness H = 0.0254 m has the initial elastic moduli C_{XX} = 920 MPa, C_{ZZ} = 100 MPa, C_{XZ} = 100 MPa, and G = 30 MPa. Fig. 9 illustrates the effect of anisotropy of the inner layer on the FRF of the beam. As seen, in this case, only a change in the shear modulus G_I of the inner layer significantly affected the FRF.

The data in Fig. 10 illustrate the effect of anisotropy of the outer layer of the beam on its FRF.

A numerical analysis showed that only a change in the modulus C_{XX} of the outer, rigid layers did affect the FRF of the layered beam noticeably. It should be noted that the influence of their shear modulus G_f (see Fig. 10) was insignificant. A similar picture was also observed for the elastic constants C_{XZ} and C_{ZZ}.

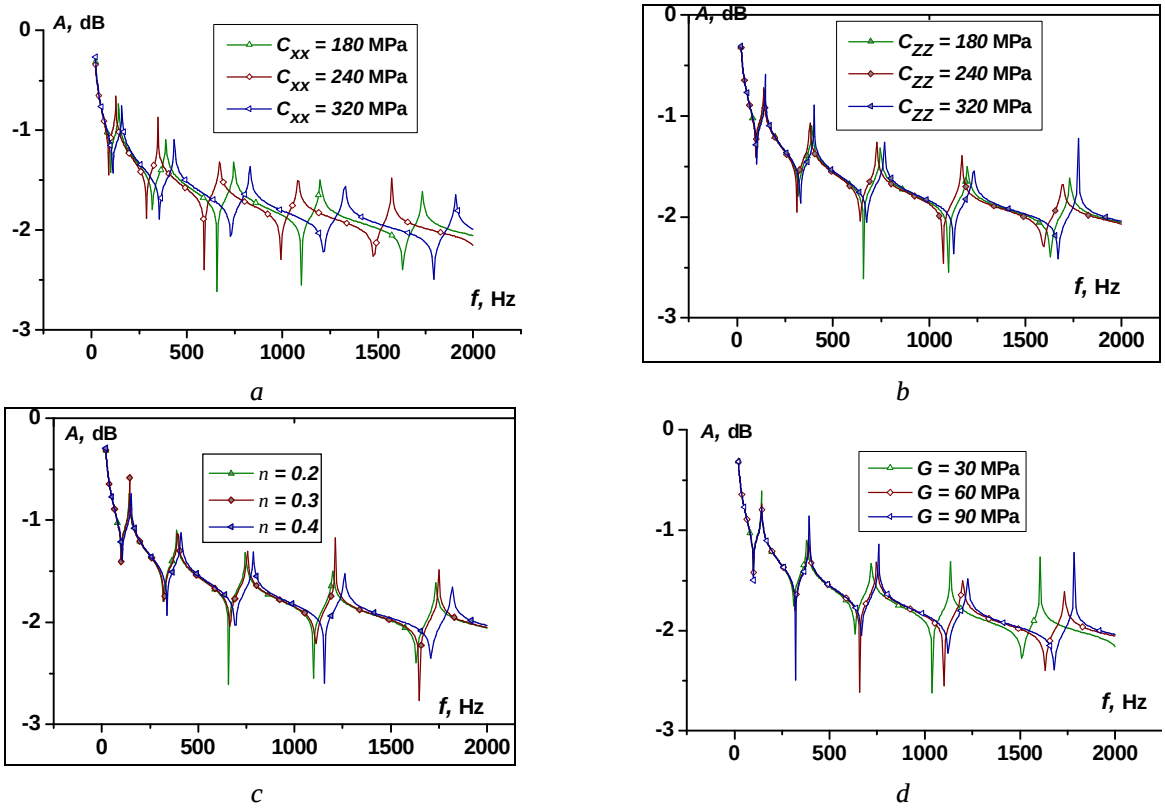

Fig. 8. *FRFs for the elastic constants of the inner layer: C_{xx} (a); C_{zz} (b); C_{xz} (c) and G (d)*

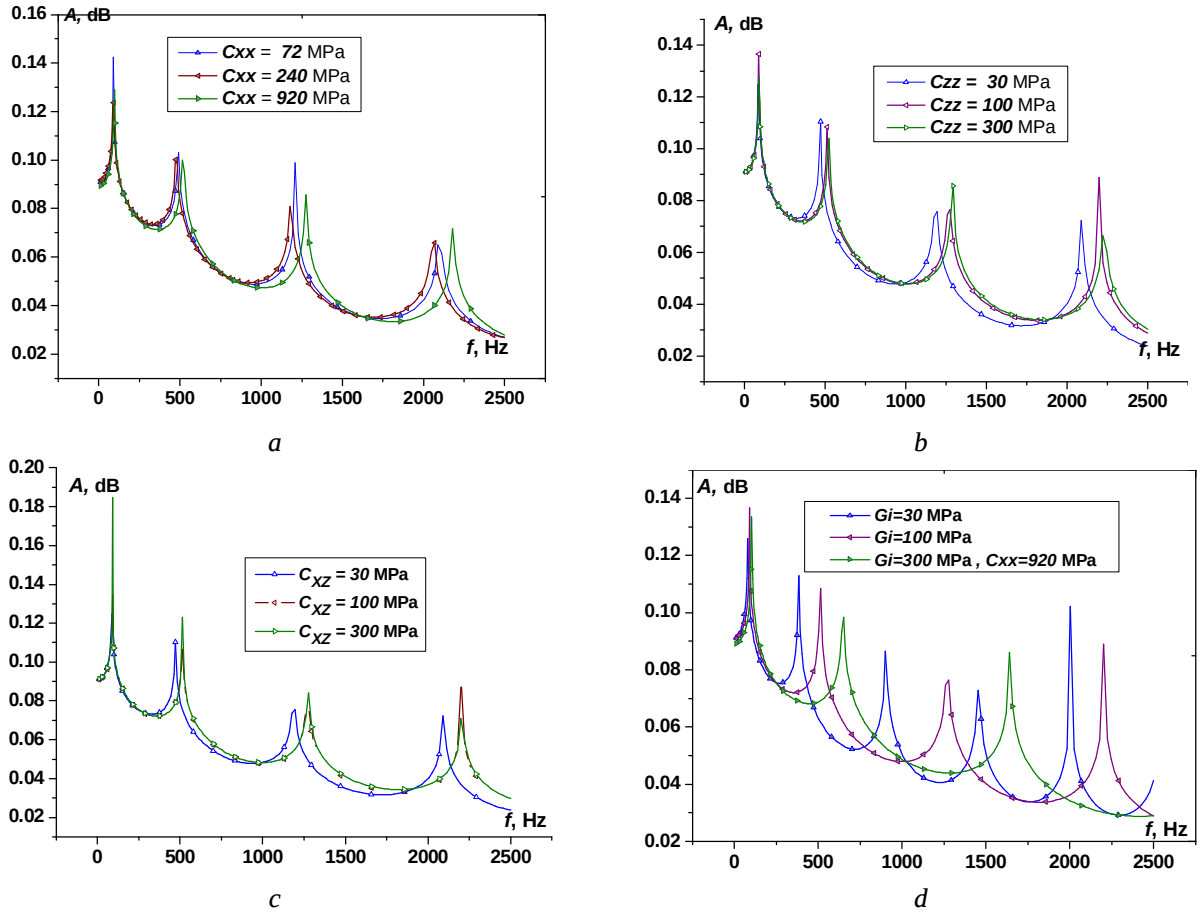

Fig. 9. *FRFs for the elastic constants of the inner layer: C_{xx} (a); C_{zz} (b); C_{xz} (c) and G (d)*

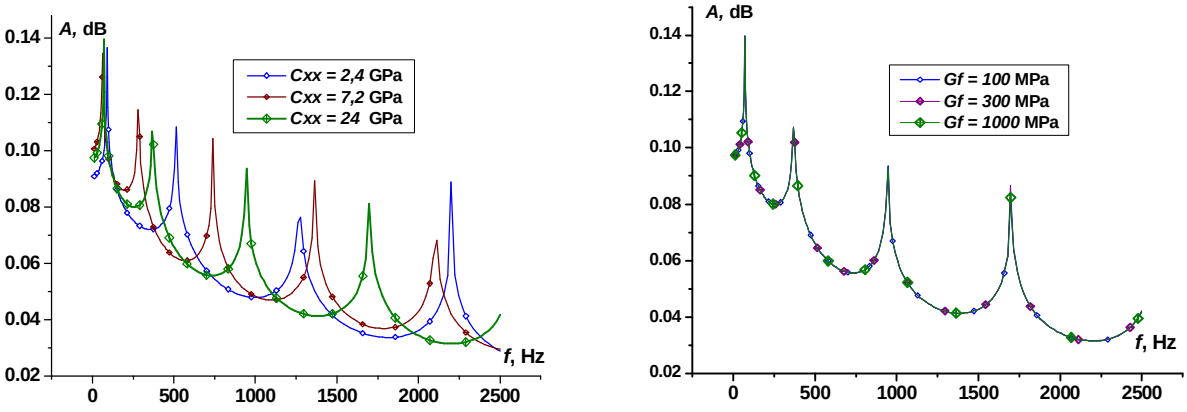

a *b*

Fig. 10. *FRFs for the elastic constants of the outer layer:* C_{xx} *(a);* G *(b)*

Damping properties in the frequency domain

Analogue theories and order-dependent results may be obtained also for the prediction of damping [39-41]. This result may be achieved by direct computation by use of the stiffness matrix if the damping matrix is congruent to the stiffness matrix.

$$C(S,V,s)=\left(a_1\cdot\left(\frac{N(S,V,s)-N_{\min}}{N_{\max}-N_{\min}}\right)+a_2\cdot\left(\frac{\Pi(S,V)-\Pi_{\min}}{\Pi_{\max}-\Pi_{\min}}\right)\right), \tag{22}$$

where $[K]$ is the stiffness matrix, $|q|$ is a vector of displacement components, $[K_i]$ is a stiffness matrix component corresponding to (i^{th}) layer ($[K]=\sum_i [K_i]$). Components of damping matrix C are usually taken proportional to components of the rigidity matrix: $C_i = h_i[K_i]$. In the previous section of this paper, the frequency influence on the properties of sandwich panels may be seen. For this purpose, fewer investigations were made for damping properties investigation in the frequency domain.

Near the FRF and damping areas presented for the sandwich with the damping core ($h_i = 0, i \neq 1$) for simply supported centrally loaded beam ($f_k(x)=\sin\left((2k-1)p\,x/2L\right)$, $g_k(x)=\cos\left((2k-1)p\,x/2L\right)$) for the following geometrical parameters: length L was chosen to be 0.1 m, core thickness was chosen to be $H=0.030$ m. The core elastic moduli were assumed to be as follows: $C_{xx}=180$ MPa, $C_{zz}=150$ MPa, $G=40$ MPa, and $C_{xz}=75$ MPa (n =0.3); density $r=240\,kg/m^3$. Face layers thickness was chosen to be $H=0.002$ m. The elastic moduli were assumed to be as follows: $C_{xx}=5400$ MPa, $C_{zz}=750$ MPa, $G=200$ MPa, and $C_{xz}=375$ MPa; $r=2400\,kg/m^3$.

In the case of dynamic tests, the error function is chosen in the form of quadratic deviation of Timoshenko beam eigen-frequencies f_i^T from calculated f_i^c values of vibration eigen-frequencies:

$$F_c=\sum_i^{N_f}\left(\frac{\left|f_i^T(E_T,G_T)-f_i^c\right|}{f_i^{\exp}}\right)^2. \tag{23}$$

Here E_T, G_T is Young and shear module of an equivalent beam. The numerical calculation of vibration eigenfrequencies was performed on the basis of relations (16-21), with account of elastic and inertial properties of the beam. Fig. 11 shows the $E-G$ maps – the level lines of error function (23) upon variation of the moduli of homogeneous beams.

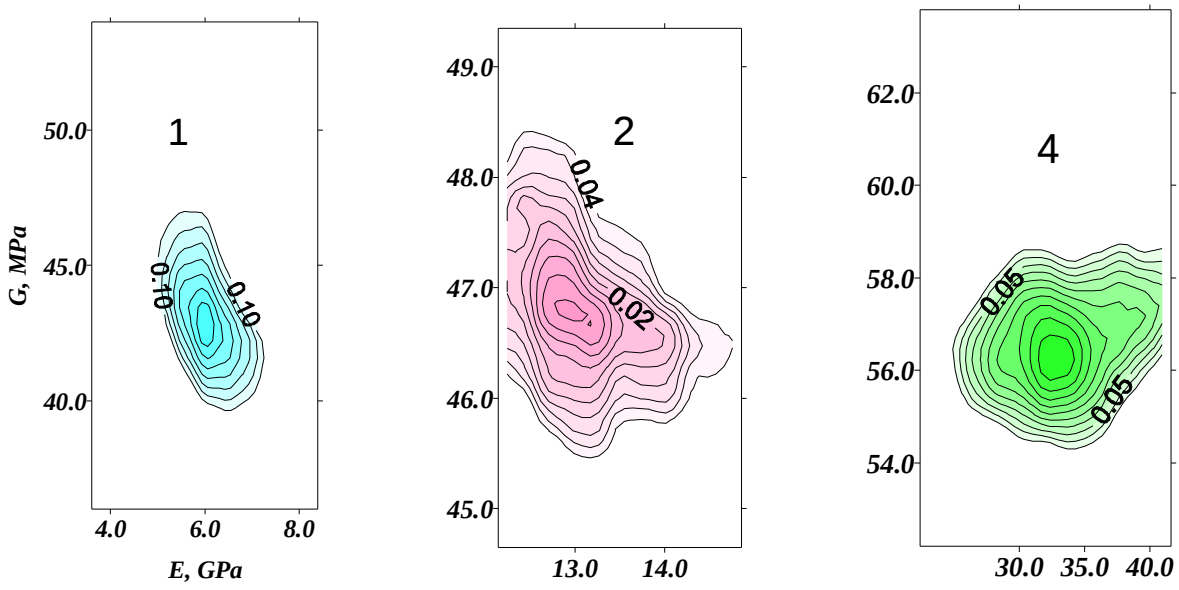

a *b* *c*

Fig. 11. *$E_T - G_T$ maps — the level lines of error function (23) upon variation of the moduli of homogeneous beams for various face sheets thickness: a – one face sheets, $H_F = 0,0005$ m; b – two face sheets, $H_F = 0,001$ m; c – four face sheets, $H_F = 0,002$ m*

In Fig. 12, sandwich beam FRF, damping and equivalent Timoshenko beam FRF are presented. Core damping was 1.2 %.

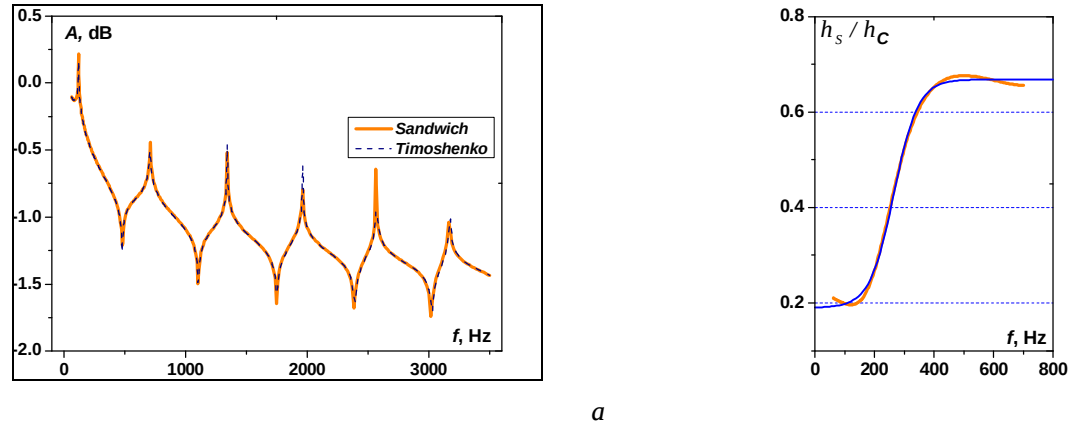

a

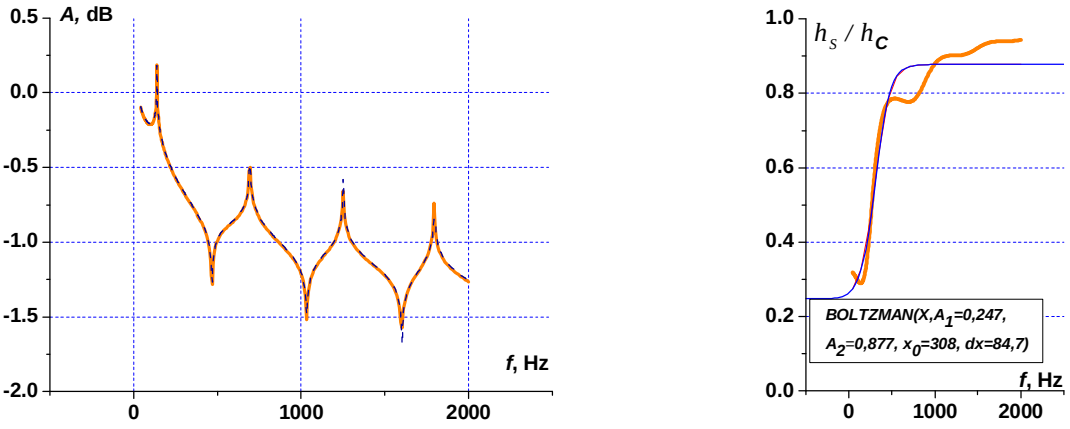

b

Fig. 12. *Sandwich beam and equivalent Timoshenko beam FRF (a); relative damping and Bolzman approximation of damping.: a – one face sheets, $H_F = 0,0005$ m; b – two face sheets, $H_F = 0,001$ m*

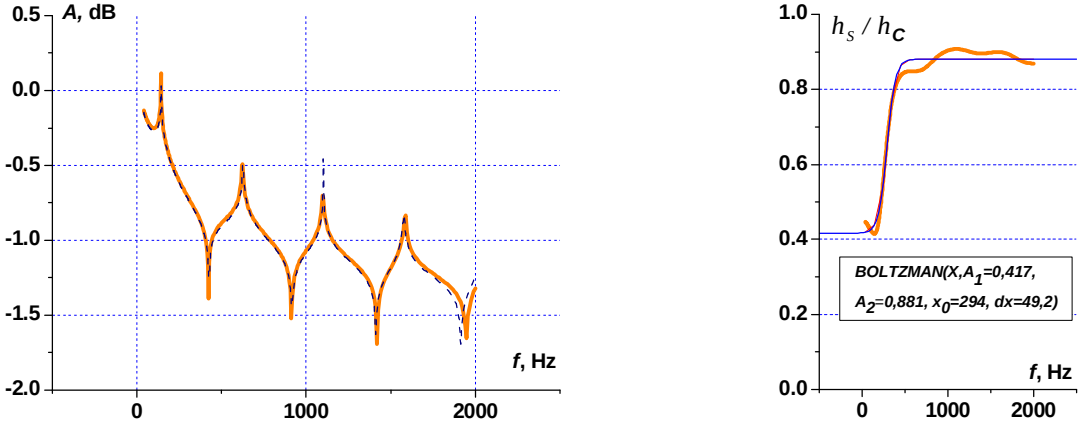

c

Continuation of fig. 12. *(c) – four face sheets,* $H_F = 0,002\ m$

Here for the relative damping h_Σ / h_C – the relation of the howl sandwich damping to the core damping the Boltzman approximation is done.

$$y = \frac{A_1 - A_2}{1 + \exp\left(x - x_0 / dx\right)}. \tag{24}$$

In Fig. 13, damping for the centrally clamped and simply supported sandwich beams with various lengths is presented.

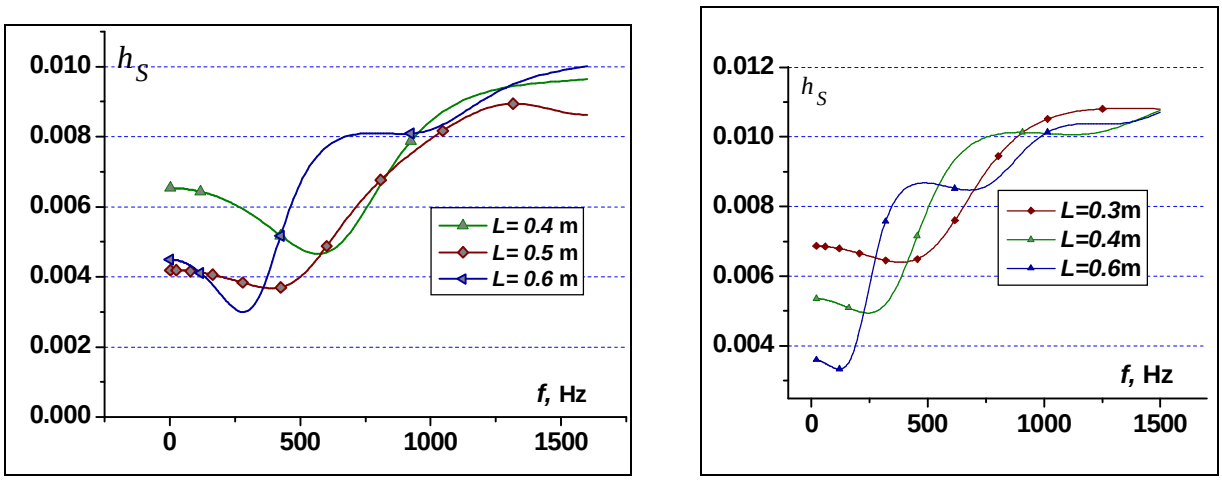

a *b*

Fig. 13. *Centrally clamped beams with the lengths* $L = 0.6,\ 0.4,\ 0.2\ m$ *(a); Simply supported beams damping (b)*

For the centrally clamped beams as for simply supported beams damping decreasing is seen at the lower frequency range.

In Fig. 14, the values of FRF and damping are presented for the symmetrical three-layered beam with the damping face sheets. The core and face layers mechanical characteristics were assumed to be identical to the face layers and core characteristics us above for sandwich.

In Fig. 15 centrally clamped beams damping with the rigid core thickness: (a) $H_C = 0.002\ m$; (b) – $H_C = 0.004\ m$ are presented.

Fig. 16 shows the $E - G$ maps – the level lines of error function (23) upon variation of the moduli of homogeneous Timoshenko beams for various face sheets thickness: (a) – $H_F = 0,001\ m$; (b) – two face sheets, $H_F = 0,001\ m$; (c) – four face sheets, $H_F = 0,002\ m$.

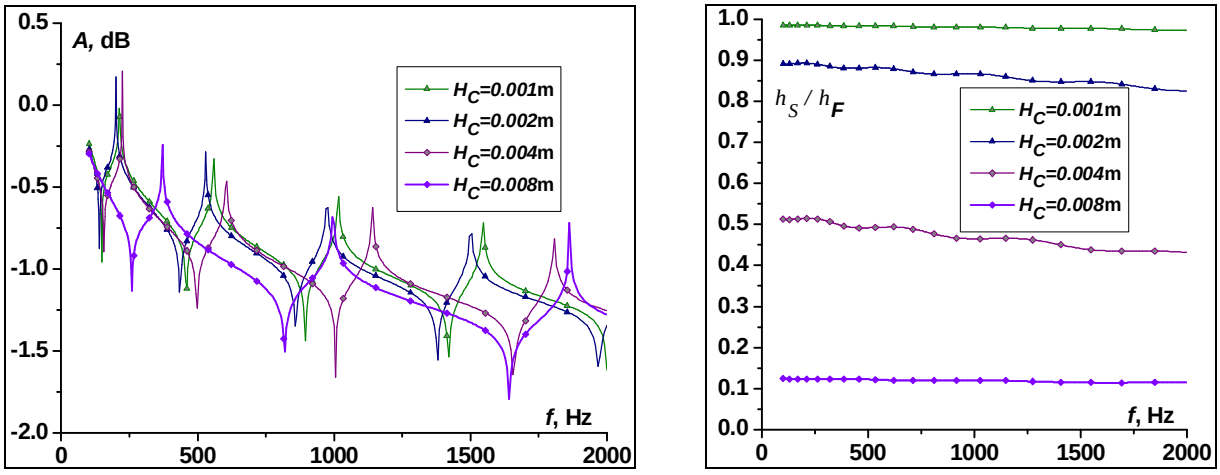

a *b*

Fig. 14. *FRF and damping for the symmetrical three-layered beam with the damping face sheets*

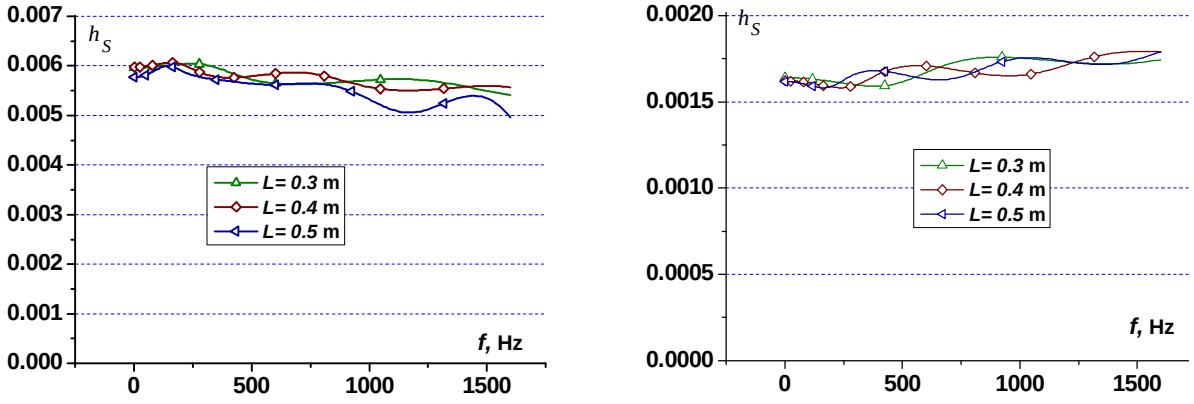

a *b*

Fig. 15. *Centrally clamped beams damping with the rigid core thickness (a):* $a - H_C = 0.002\ m$ *;* $b - H_C = 0.004\ m$

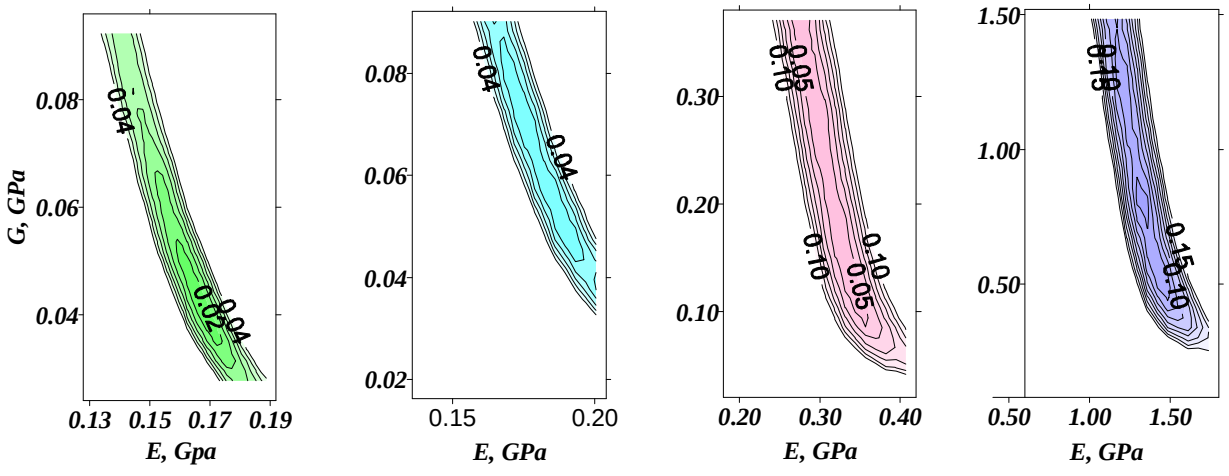

a *b* *c* *d*

Fig. 16. $E - G$ *maps – the level lines of error function (23) upon variation of the moduli of homogeneous beams for various core thickness:* $a - H_C = 0,001\ m$; $b - H_C = 0,002\ m$; $c - H_C = 0,004\ m$; $d - H_C = 0,008\ m$

In spite of sandwich beam, for the beam with thick damping face sheets the approximation by Timoshenko beam may be found only in the narrow frequency range (Fig. 17).

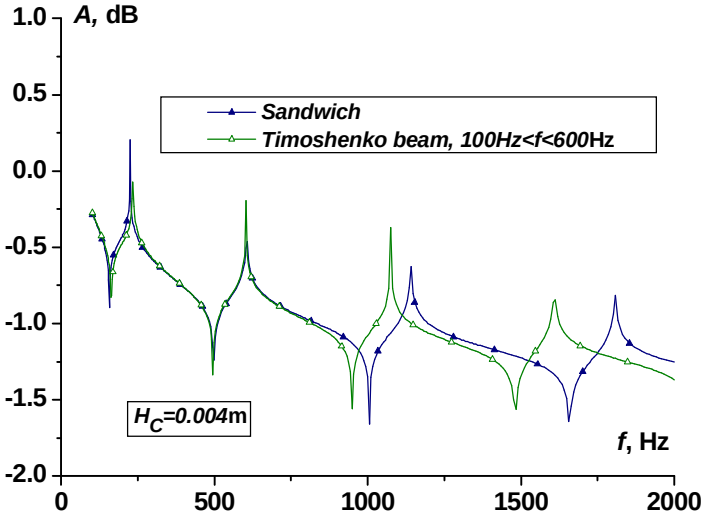

Fig. 17. *Approximation of the beam with thick damping face sheets by Timoshenko beam*

Only in the lower frequency range $100Hz < f < 600Hz$ Timoshenko beam approximate the beam with the thick soft damping face sheets. For the other frequency intervals another Timoshenko beam approximation may be found.

Fife-layered beam

In Fig.18 the values of FRF and damping are presented for the symmetrical fife-layered beam with the damping interlaminate sheets. The core and face layers mechanical characteristics were assumed to be identical to the face layers characteristics us above for sandwich and for interlaminate sheets identical to core. The values of damping of three layer beam with the soft face sheets equal thickness to damping interlaminate sheets (rhombus) are also shown.

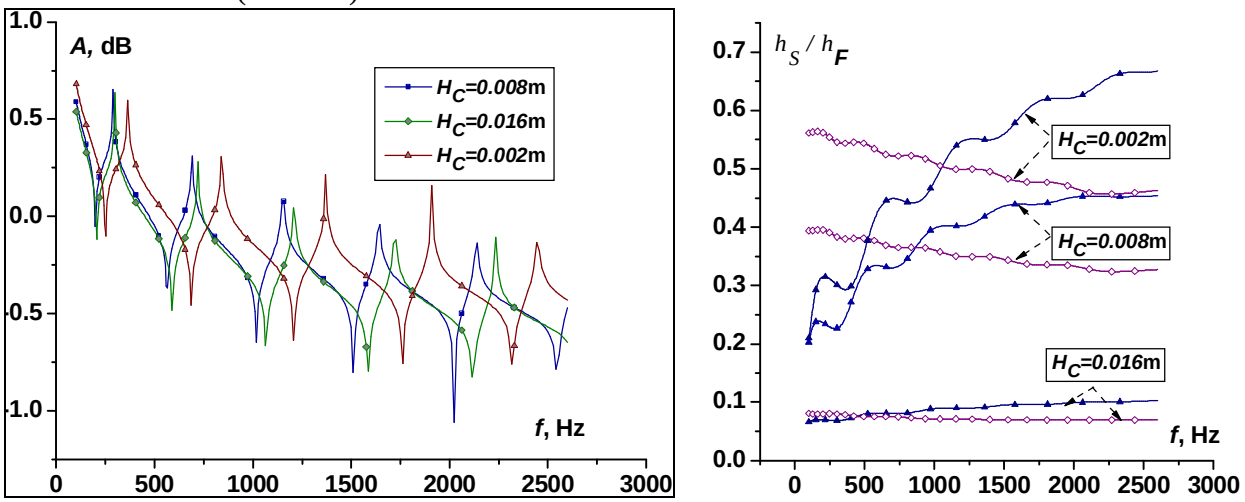

Fig. 18. *FRF and damping (triangles) for the symmetrical fife-layered beam with the damping interlaminate sheets and damping (rhombs) of three layer beam with the soft face sheets equal thickness*

In Fig. 19 the values of damping are presented for the symmetrical fife-layered beam ($2H = 0.02\ m$) with the damping various thickness interlaminate sheets (triangles) and damping of three layer beam with the soft face sheets equal thickness. Interlaminate sheets damping was $h = 1$ %. Rigid inner face sheets – $h = 0.1$ %.

For the smaller thickness H_{DEMP} of the interlaminate sheets damping in the symmetrical fife-layered beam ($2H = 0.02\ m$) with the various damping interlaminate sheets thickness H_{DEMP} and damping (small marks) of three layer beam with the soft face sheets equal thickness are presented.

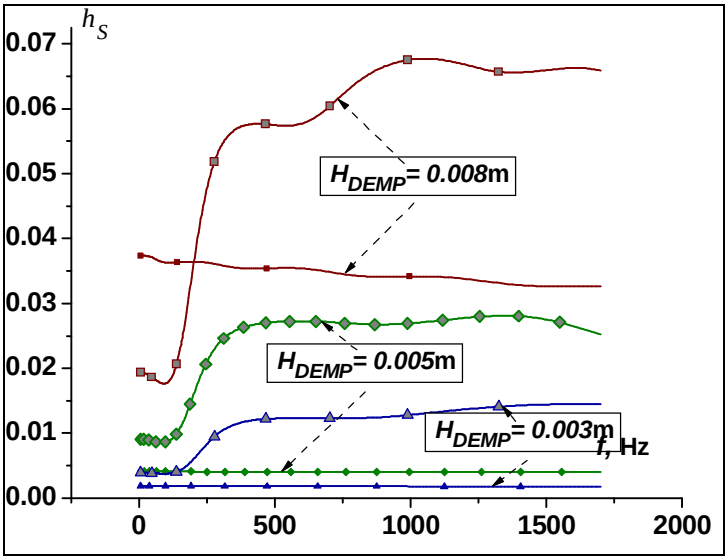

Fig. 19. *Damping in the symmetrical fife-layered beam (2H=0.02 m) with the various damping interlaminate sheets thickness* H_{DEMP} *and damping (small marks) of three layer beam with the soft face sheets equal thickness*

As expected, the damping in the beam with the constrained damping sheets is higher. Only for the thick damping sheets, the damping of the fife-layered beam is less than in three-layered beam in the lower frequency range (Fig. 18, 19).

In [42] it is shown that clamped end conditions seem to imply a higher apparent loss factor than the simply supported case, and free end conditions seem to imply a lower loss factor. In Fig. 20 damping is presented for free supported and centrally clamped beams.

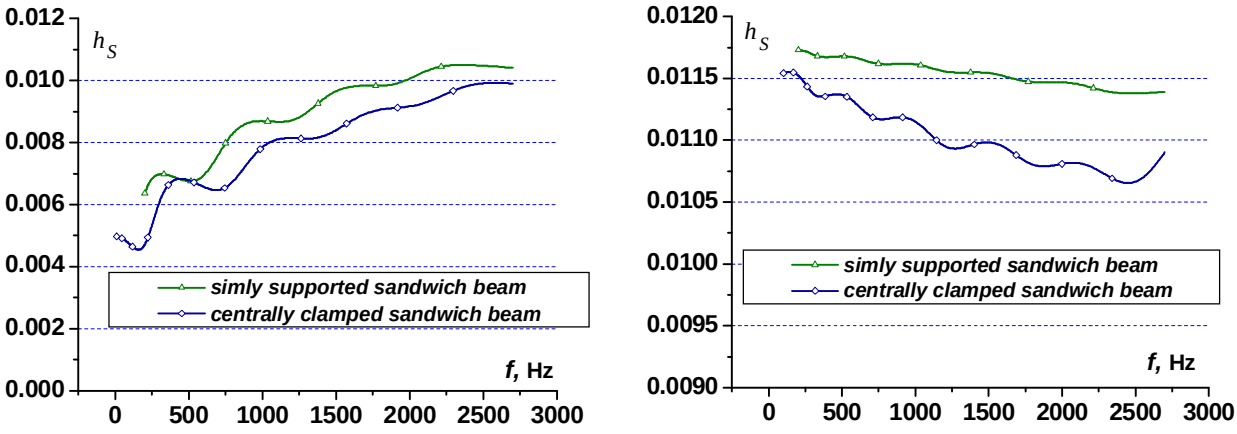

a *b*

Fig. 20. *Damping for free supported and centrally clamped beams: a – beams with the damping core,* $H_C = 0.0254\ m$; *b – damping thick face layers,* $H_C = 0.001\ m$

In spite of [42] here damping in the free supported beam is higher than in centrally clamped beam.

In [43] the through-thickness modal response of a [0/f/0] sandwich beam with Gl/Pl composite faces and foam core was studied. The beam was 0.50 m long, had a thickness 0.035m. In Fig. 21 sandwich beam FRF and damping are presented. Here *x* is a point of measuring on the length of the beam.

Fig. 22 shows distributions of the interlaminar strain, respectively, through the thickness at L=0.125m at the frequencies (*500, 1000, 1455* Hz) at FRF intersection of horizontal line (*A=-1.4*, Fig. 17, a) for the following parameters: the core elastic moduli were assumed to be as follows [43]:

$C_{xx}=35, C_{zz}=35$ MPa, $G=12$ MPa, and $C_{xz}=12$ MPa (n =0.4); density $r=45\,kg/m^3$. Face layers thickness was chosen to be $H=0.0025$ m. The elastic moduli were assumed to be as follows: $C_{xx}=8700$ MPa, $C_{zz}=8700$ MPa, $G=3500$ MPa, and $r=1672\,kg/m^3$. The core damping $h_C=0.03$, face layers damping $h_F=0.0065$.

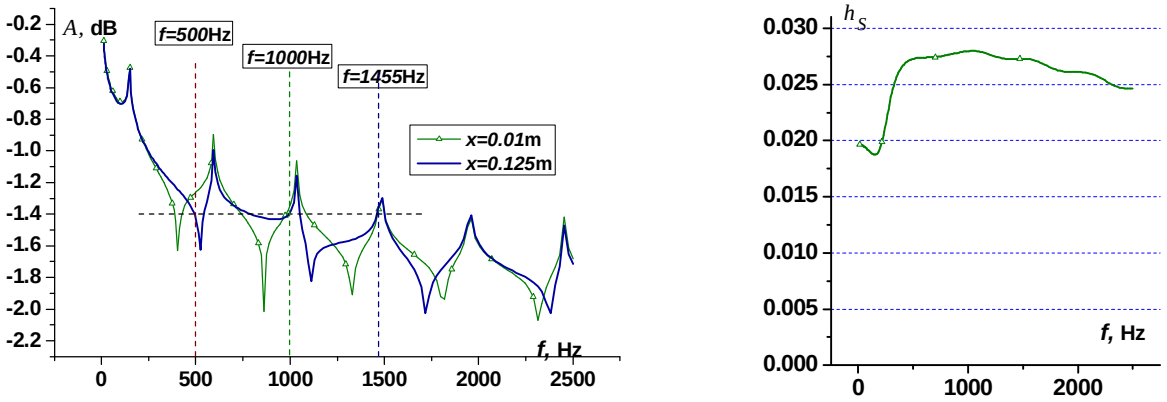

a *b*

Fig. 21. *Sandwich beam FRF (a) and damping (b)*

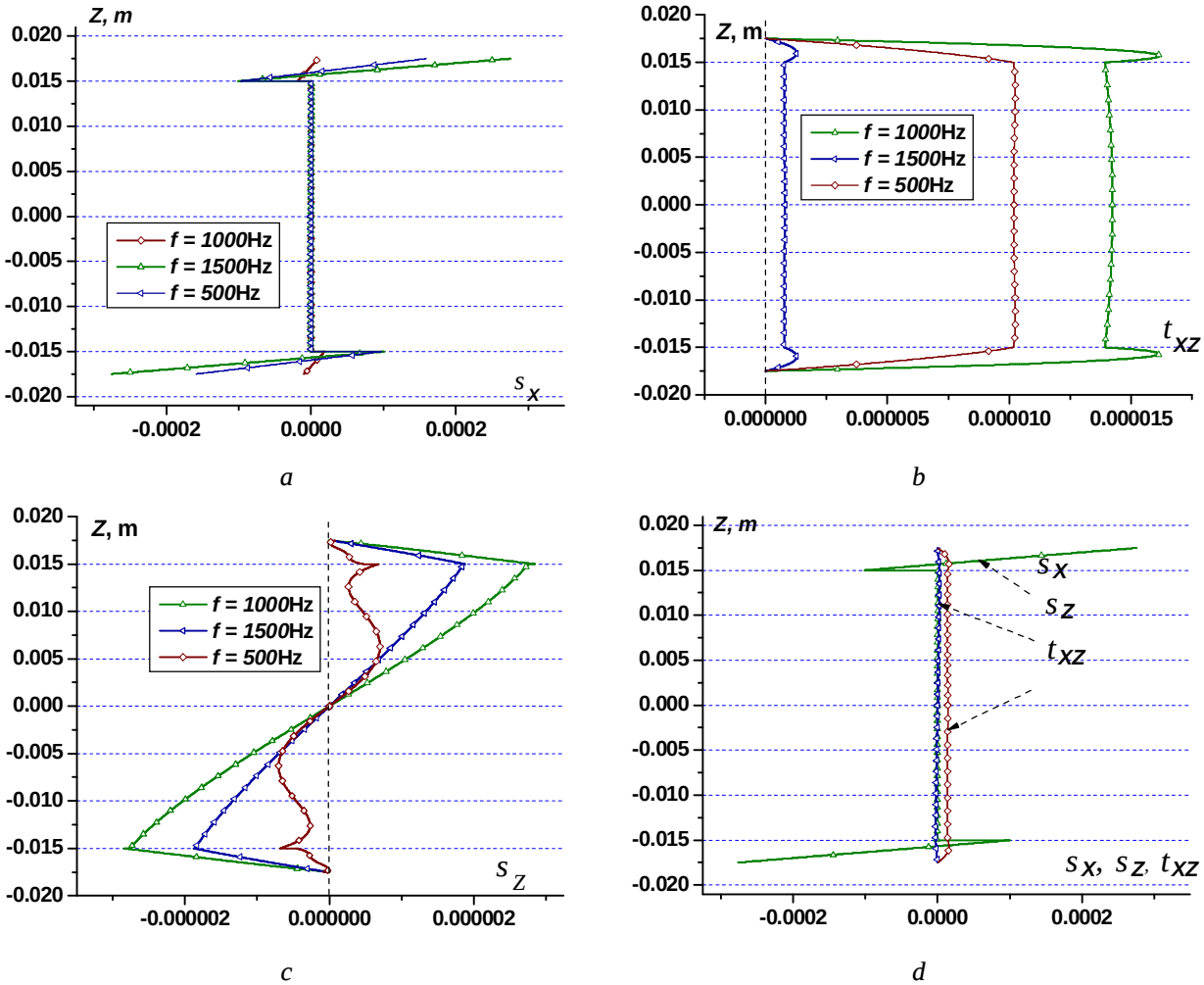

a *b*

c *d*

Fig. 22. *Distributions of the interlaminar strain, respectively, through the thickness at L=0.125 m: a – s_X ; b – t_{XZ} ; c – s_Z ; d – all stresses at f = 1000 Hz*

In [43] for the face three layers face sheets [0/f/0] three layers FEM approximation was applied. It seems to be superfluous for the relative thin rigid face sheets. As been shown above (Fig. 10) only the longitudinal face sheets module influence on the sandwich FRF. Distinct face sheets layers longitudinal moduli may be summarized as an arithmetical mean of sublayers or found by translation to the 1-order theory of Timoshenko beam, as above. In spite of FEM in [43], the approximations of order $N_Z \geq 3$ give not only the transversal stress distribution with boundary zero values, but also continuous on interlaminates lines and smooth.

High frequency diapason

In Fig. 23, influence of the theoretical order N_Z on the damping prediction accuracy in the high frequency diapason is presented for the sandwich with the damping core ($h_i = 0, i \neq 1$) for different orders of approximations in (16,17). for simply supported centrally loaded beam ($f_k(x) = \sin\left((2k-1)p\,x / 2L\right)$, $g_k(x) = \cos\left((2k-1)p\,x / 2L\right)$) for the following geometrical parameters: length L was chosen to be 0.1 m, core thickness was chosen to be $H = 0.030$ m. The core elastic moduli were assumed to be as follows: $C_{xx} = 180$ MPa, $C_{zz} = 150$ MPa, $G = 40$ MPa, and $C_{xz} = 75$ MPa (n =0.3); density $r = 240\,kg/m^3$. Face layers thickness was chosen to be $H = 0.002$ m. The elastic moduli were assumed to be as follows: $C_{xx} = 5400$ MPa, $C_{zz} = 750$ MPa, $G = 200$ MPa, and $C_{xz} = 375$ MPa; $r = 2400\,kg/m^3$.

Here h_Σ / h_C is the ratio of the whole damping of sandwich to the damping in core layer. The behavior of these curves is not similar to the ones in the lower frequency range. For the sandwich beam with thick damping core, the damping is seen to decrease just above 1,700 Hz.

In Fig. 24, the values of damping is presented for the symmetrical three-layered beam with the damping face sheets ($h_i = 0, i = 1$) (us above the influence of the orders of approximations in (16,17) is practically equivalent for $N_Z \geq 2$). Here core thickness was chosen to be $H = 0.008$ m, face layers thickness was $H = 0.016$ m. The core and face layers mechanical characteristics were assumed to be identical to the face layers and core characteristics us above for sandwich. Damping fluctuations also may be seen. Now consider this region in more detail.

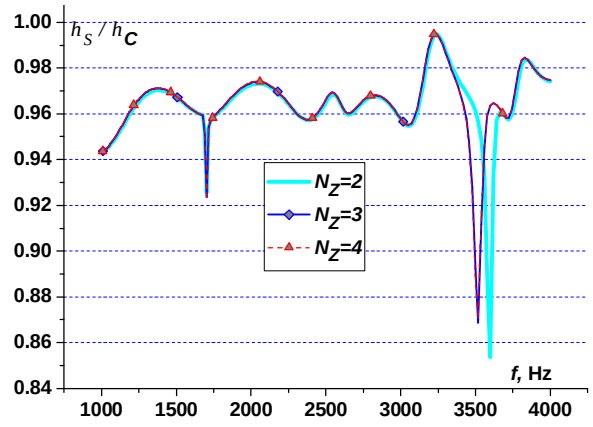

Fig. 23. *Relative damping h_Σ / h_C fluctuations (sandwich)*

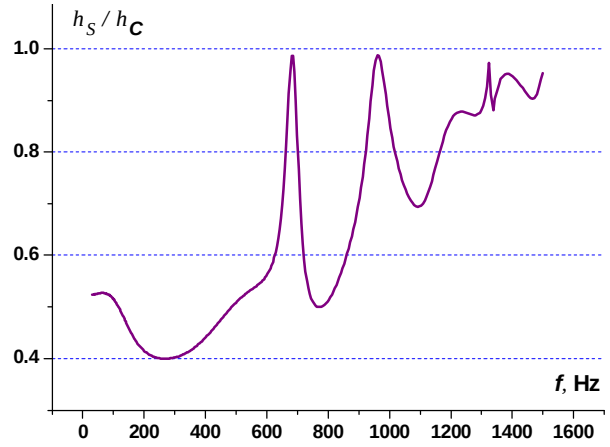

Fig. 24. *Relative damping h_Σ / h_C fluctuations (soft face sheets)*

In Fig. 25 stress distributions through one-half of the beam thickness are presented for this symmetrical beams in the region of the damping fluctuations (f = 680 Hz) and in the region of small damping (f = 250 Hz).

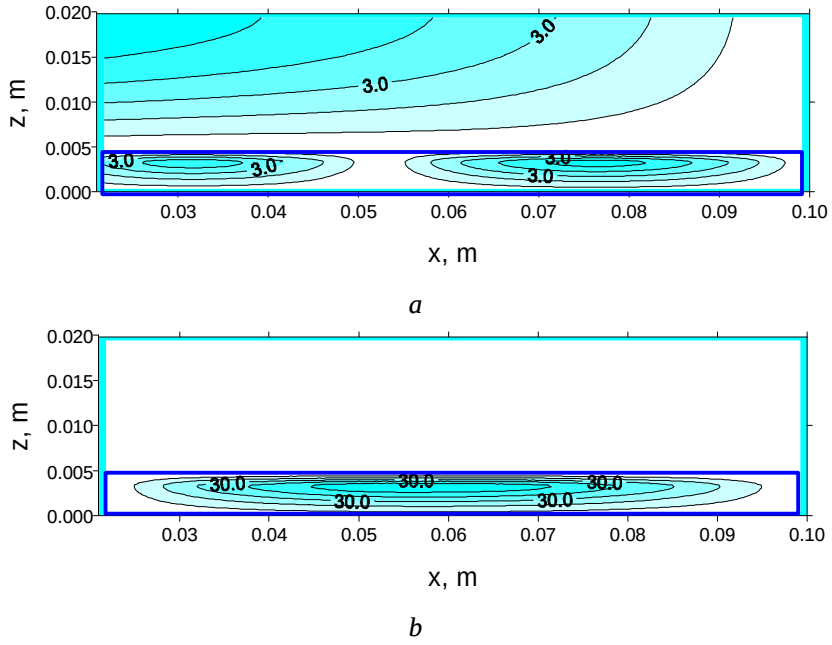

Fig. 25. *Normal stress* s_X *distributions through one-half of the beam thickness: a – in the region of the damping fluctuations (f = 685 Hz); b – near f = 250 Hz*

It can be seen in Fig. 25, *b*, that the stresses in the damping layer (damping is nonzero only in the face layers: 4 mm < H < 20 mm) are small compared to the stresses presented in Fig. 25, *a*.

Elastically fixed cantilever beam

Finally, let us consider a homogeneous orthotropic elastically fixed cantilever beam, important in many technical applications (Fig. 26).

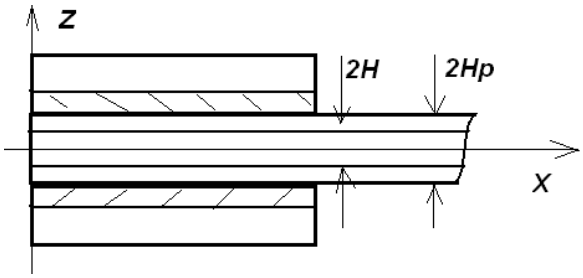

Fig. 25. *Plate in an elastic holder*

The equations of dynamic equilibrium are obtained by inserting Eqs. (2) and kinematic approximations (16) and (17) into the Hamilton–Ostrogradski variational equation with an elastic fastening of Winckler type with a modulus of subgrade reaction K

$$\int_{t_1}^{t_2}\left(\int_V (s_{xx}de_{xx}+s_{zz}de_{zz}+t_{xz}de_{xz}-r\frac{\partial u}{\partial t}d\frac{\partial u}{\partial t}-r\frac{\partial w}{\partial t}d\frac{\partial w}{\partial t})dV+\int_{S_K} KUdUdS-\int_{S_P} PdUdS\right)dt=0. \qquad (25)$$

where V is the volume of the plate, S_K is the surface of the elastic fastening, S_P is the surface with known forces, and $[t_1, t_2]$ is an hour interval.

Let us first consider a homogeneous orthotropic elastically fixed cantilever beam with L = 0.3 m and H = 0.0127 m. The elastic characteristics of the beam material (MPa) are C_{XX} = 160, C_{ZZ} = 160, G = 35, and C_{XZ} = 60. Fig. 27 depicts the diagrams the first three eigen-frequencies f_i as functions of the rigidity K of the elastic fastening. The eigen-frequencies of the beam f_i are found on the basis of Eqs. (16)-(21). In calculating the eigen-frequencies according to the method described, the coordinate functions

were given by the trigonometric functions $f(x) = g_k(x) = \sin\left(kpx/2L\right)$ (see Appendix B). The calculation results presented in Fig. 27 show that, in the case of strong anisotropy (G is decreased tenfold), the influence of the parameters of rigid fixation is considerably more pronounced. The calculation results presented in [20] show that, in the case of strong anisotropy C_{XX} is increased tenfold), the influence of the parameters of rigid fixation is considerably more pronounced, and the region of maximum normal strains is greater. This is illustrated in Fig. 27, b. Here the length of fastening is L = 0.05 m. In Fig. 27, the eigen-frequencies f_i as functions of the rigidity K of the elastic fastening and bounds of this frequencies are presented for beam without the elastic fastening of length L = 0.3 m, L = 0.25 m. The upper bound is the eigen-frequency of shot beam – beam mines clamping zone.

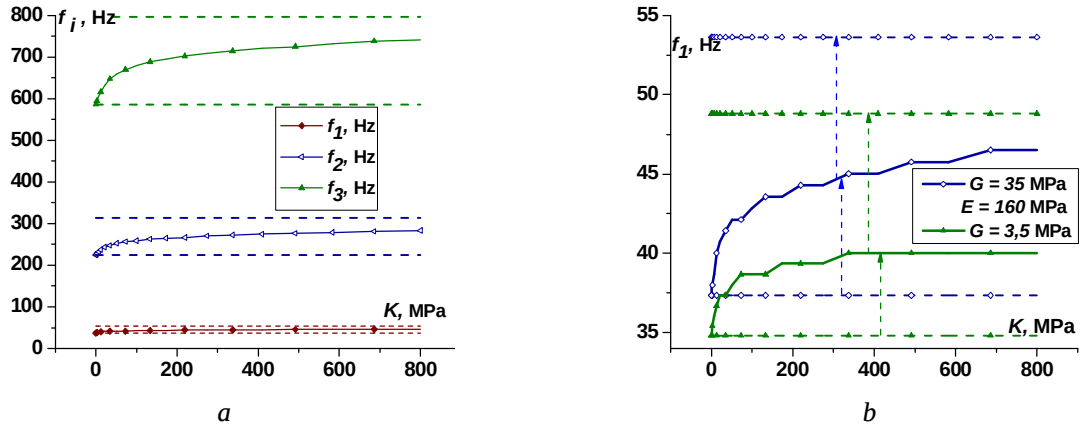

a *b*

Fig. 27. *First three eigen-frequencies f_i as functions of the rigidity K of the elastic fastening (a); Influence of beam anisotropy on the first eigen-frequency f_1 (b)*

In Fig. 28, *a–c* the analogues values for the thinner beam (H = 0.00635 m) are presented. Here, vertical signs present the bounds calculated for the Timoshenko theory.

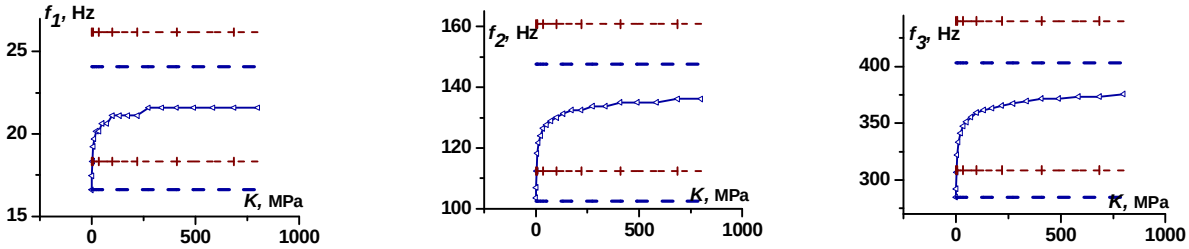

a *b* *c*

Fig. 28. *The analogues values for the thinner beam (H = 0.00635 m)*

First three eigen-frequencies f_i as functions of the rigidity K of the elastic sandwich fastening are shown in Fig. 29, *a–c*. The results are presented for various friction coefficients k_T in the clamp region.

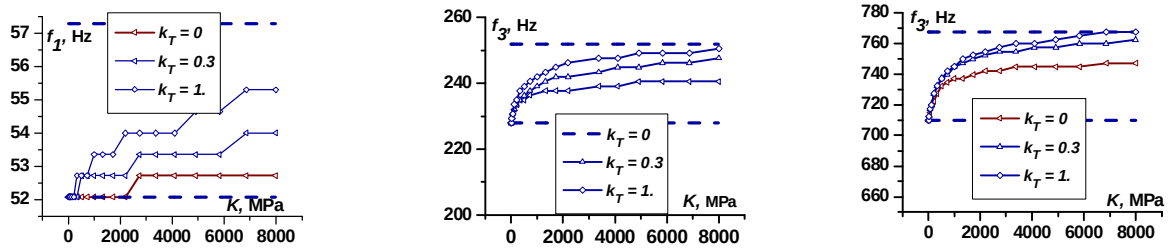

a *b* *c*

Fig. 29. *First three eigen-frequencies f_i as functions of the rigidity K of the elastic fastening*

In Fig. 30, *a–c* first three beam eigen-frequencies f_i as functions of the rigidity K of the elastic three-layered soft face layers beam with the fastening are shown. Mechanical properties of the soft layers are as above. The elastic characteristics of the beam the rigid layers material (MPa) are C_{XX} = 9120, C_{ZZ} = 480 , G = 145, and C_{XZ} = 180. Here, as evidently, the influence of fastening is greater. For clamped sandwich the first eigen-frequency variation for the clamp without friction is small.

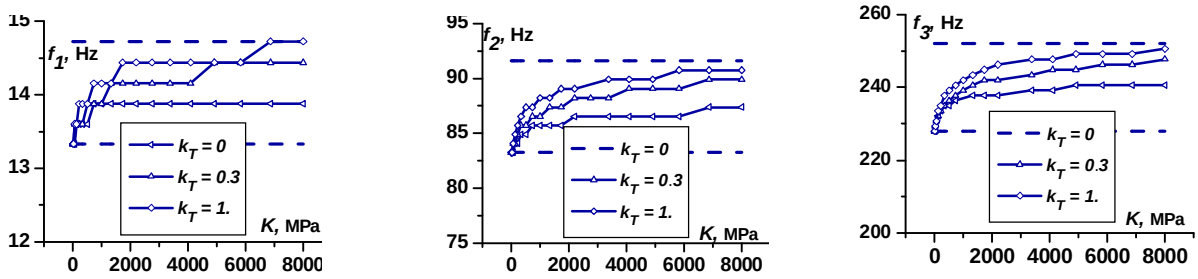

Fig. 30. *First three eigen-frequencies f_i as functions of the rigidity K of the elastic fastening*

Let us consider now the damping in sandwich and the three-layered beam with the thick soft layers damping vs the rigidity of the elastic fastening K (Fig. 31). Here the additional damping in elastic clamp may be found as for the beam by (22). For the elastic fastening as Winkler foundation additional deformation energy is $U_{CLAMP} = \int_0^{L_Z} K\, w^2(x,H)/2\, dx$ and the additional losses are $U_{CLAMPloss} = h_{CLAMP} \int_0^{L_Z} K\, w^2(x,H)/2\, dx$. The first term must be added to denominator and second to numerator for the clamp damping account in (22). In Fig. 31 the damping increasing with the rigidity increasing of damping clamp may be seen. For the values of K grater than *100* MPa the summary damping is increasing. Here the rubber made clamp layers damping is $h_C = 0{,}3$. As for the sandwich so for the beam with the thick face soft layers the damping increasing with the rigidity increasing of damping clamp may be seen, but only to some value of K.

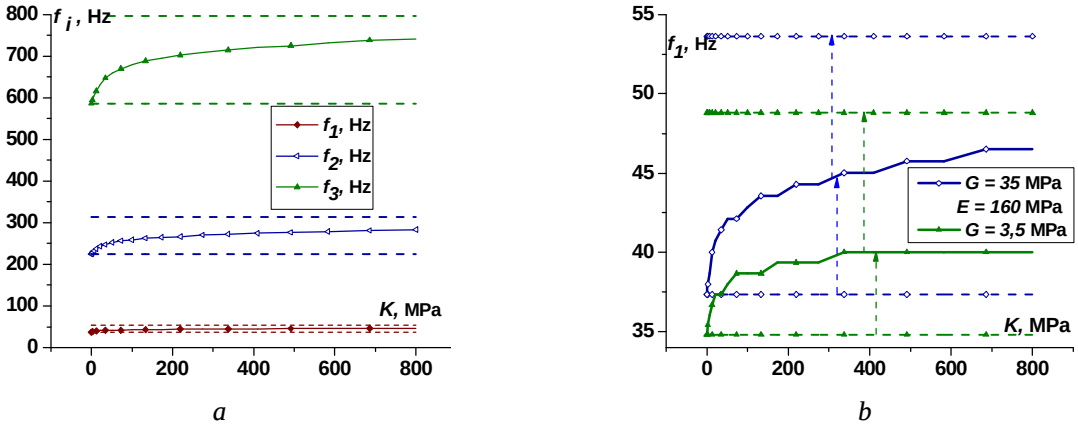

Fig. 31. *Elastically clamped beams vs the rigidity of the elastic fastening rigidity E_k and damping in fastening layers – $h_C = 0{,}3$: a –sandwich beam; b – three-layered beam with the thick face soft layers*

Conclusions

Theoretical models for the dynamics and damping of laminated structures have been developed. With the small number of parameters studied so far this approach predicts the dynamic behavior of the beams investigated. Using this model for layered beams, higher order modeling was carried out, not only for the damping caused by the shear strain in the core, but also for the damping caused by normal and bending deformation. This is important for the middle and high frequency analysis of the damping

properties of sandwich structures. The main advantage of the present method is that it does not rely on strong assumptions about the model of the plate. The key feature is that series of models can be applied for different vibration conditions of the plate by use of a suitable analytical or approximate method. Different cases of beam fastening were examined. Important in many technical applications elastically fixed cantilever beam, was under discussion. The summary damping of the stratification was found for various damping layers distribution for various beams fastening in the wide frequency range, among them taking into account damping in a clamp. By the numerical experiment very near results for adaptive numerical schemes of lower approximation degree in normal direction are established. The equivalent Timoshenko beam for an arbitrary layered beam was found. For the sandwich type beam an equivalent beam may be found with dynamic properties practically identical in the wide frequency range. Found equivalent Timoshenko beams may be applied in many numerical technical applications: in the dynamic vibroprotecting and vibroabsorbing systems, in the lower frequency sound insulation systems.

Appendix A. The structure of a system matrix

The vector of the unknown parameters is

$$U=\begin{pmatrix} u_{11}^{e},u_{12}^{e},...,u_{1N_x}^{e},w_{11}^{e},w_{12}^{e},...,w_{1N_x}^{e};u_{21}^{e},u_{22}^{e},...,u_{2N_x}^{e},w_{21}^{e},w_{22}^{e},...,w_{2N_x}^{e};... \\ u_{N_z1}^{e},u_{N_z2}^{e},...,u_{N_zN_x}^{e},w_{N_z1}^{e},w_{N_z2}^{e},...,w_{N_zN_x}^{e}; \\ u_{11}^{d},u_{12}^{d},...,u_{1N_x}^{d},w_{11}^{d},w_{12}^{d},...,w_{1N_x}^{d};u_{21}^{d},u_{22}^{d},...,u_{2N_x}^{d},w_{21}^{d},w_{22}^{d},...,w_{2N_x}^{d};... \\ u_{N_z1}^{d},u_{N_z2}^{d},...,u_{N_zN_x}^{d},w_{N_z1}^{d},w_{N_z2}^{d},...,w_{N_zN_x}^{d}. \end{pmatrix}. \quad \text{(A1)}$$

Matrices of integrals of the products of the longitudinal functions are:

$$\left[A_1^X\right]=\begin{bmatrix} \int_0^L f_1(x)f_1(x)dx & \int_0^L f_1(x)f_2(x)dx & ... & \int_0^L f_1(x)f_{N_X}(x)dx \\ \int_0^L f_2(x)f_1(x)dx & \int_0^L f_2(x)f_2(x)dx & ... & \int_0^L f_2(x)f_{N_X}(x)dx \\ ... & ... & ... & ... \\ \int_0^L f_{N_X}(x)f_1(x)dx & \int_0^L f_{N_X}(x)f_2(x)dx & ... & \int_0^L f_{N_X}(x)f_{N_X}(x)dx \end{bmatrix},$$

$$\left[A_{1P}^X\right]=\begin{bmatrix} \int_0^L f_1(x)f_1'(x)dx & \int_0^L f_1(x)f_2'(x)dx & ... & \int_0^L f_1(x)f_{N_X}'(x)dx \\ \int_0^L f_2(x)f_1'(x)dx & \int_0^L f_2(x)f_2'(x)dx & ... & \int_0^L f_2(x)f_{N_X}'(x)dx \\ ... & ... & ... & ... \\ \int_0^L f_{N_X}(x)f_1'(x)dx & \int_0^L f_{N_X}(x)f_2'(x)dx & ... & \int_0^L f_{N_X}(x)f_{N_X}'(x)dx \end{bmatrix}, \quad \text{(A2)}$$

$$\left[A_{1PP}^X\right]=\begin{bmatrix} \int_0^L f_1'(x)f_1'(x)dx & \int_0^L f_1'(x)f_2'(x)dx & ... & \int_0^L f_1'(x)f_{N_X}'(x)dx \\ \int_0^L f_2'(x)f_1'(x)dx & \int_0^L f_2'(x)f_2'(x)dx & ... & \int_0^L f_2'(x)f_{N_X}'(x)dx \\ ... & ... & ... & ... \\ \int_0^L f_{N_X}'(x)f_1'(x)dx & \int_0^L f_{N_X}'(x)f_2'(x)dx & ... & \int_0^L f_{N_X}'(x)f_{N_X}'(x)dx \end{bmatrix}.$$

The same forms have matrices $\left[B_{1P}^X\right]$, $\left[B_{1P}^X\right]$, $\left[B_{1P}^X\right]$, only functions $f_k(x)$ must be substituted by $g_k(x)$. Matrices $\left[AB_1^X\right]$,$\left[APB_1^X\right]$,$\left[ABP_1^X\right]$ (mixed) are defined such

$$\left[AB_1^X\right]=\begin{bmatrix} \int_0^L f_1(x)g_1(x)dx & \int_0^L f_1(x)g_2(x)dx & \dots & \int_0^L f_1(x)g_{N_X}(x)dx \\ \int_0^L f_2(x)g_1(x)dx & \int_0^L f_2(x)g_2(x)dx & \dots & \int_0^L f_2(x)g_{N_X}(x)dx \\ \dots & \dots & \dots & \dots \\ \int_0^L f_{N_X}(x)g_1(x)dx & \int_0^L f_{N_X}(x)g_2(x)dx & \dots & \int_0^L f_{N_X}(x)g_{N_X}(x)dx \end{bmatrix},$$

$$\left[APB_1^X\right]=\begin{bmatrix} \int_0^L f_1(x)g_1'(x)dx & \int_0^L f_1(x)g_2'(x)dx & \dots & \int_0^L f_1(x)g_{N_X}'(x)dx \\ \int_0^L f_2(x)g_1'(x)dx & \int_0^L f_2(x)g_2'(x)dx & \dots & \int_0^L f_2(x)g_{N_X}'(x)dx \\ \dots & \dots & \dots & \dots \\ \int_0^L f_{N_X}(x)g_1'(x)dx & \int_0^L f_{N_X}(x)g_2'(x)dx & \dots & \int_0^L f_{N_X}(x)g_{N_X}'(x)dx \end{bmatrix},$$

$$\left[ABP_1^X\right]=\begin{bmatrix} \int_0^L f_1'(x)g_1(x)dx & \int_0^L f_1'(x)g_2(x)dx & \dots & \int_0^L f_1'(x)g_{N_X}(x)dx \\ \int_0^L f_2'(x)g_1(x)dx & \int_0^L f_2'(x)g_2(x)dx & \dots & \int_0^L f_2'(x)g_{N_X}(x)dx \\ \dots & \dots & \dots & \dots \\ \int_0^L f_{N_X}'(x)g_1(x)dx & \int_0^L f_{N_X}'(x)g_2(x)dx & \dots & \int_0^L f_{N_X}'(x)g_{N_X}(x)dx \end{bmatrix}.$$

Let us consider first one layer. Now the common matrix of the system (21) has the form

$$[A]=\begin{bmatrix} [A_{uu}]-w^2[A_{mu}] & [A_{uw}] \\ [A_{wu}] & [A_{ww}]-w^2[A_{mu}] \end{bmatrix}. \qquad \text{(A3)}$$

Here

$$[A_{uu}]=\begin{bmatrix} \left[A_1^X\right]g_{11}+\left[A_{1pp}^X\right]c_{11} & \left[A_1^X\right]g_{12}+\left[A_{1pp}^X\right]c_{12} & \dots & \left[A_1^X\right]g_{1N_Z}+\left[A_{1pp}^X\right]c_{1N_Z} \\ \left[A_1^X\right]g_{21}+\left[A_{1pp}^X\right]c_{21} & \left[A_1^X\right]g_{22}+\left[A_{1pp}^X\right]c_{22} & \dots & \left[A_1^X\right]g_{2N_Z}+\left[A_{1pp}^X\right]c_{2N_Z} \\ \dots & \dots & \dots & \dots \\ \left[A_1^X\right]g_{N_Z1}+\left[A_{1pp}^X\right]c_{N_Z1} & \left[A_1^X\right]g_{N_Z2}+\left[A_{1pp}^X\right]c_{N_Z2} & \dots & \left[A_1^X\right]g_{N_ZN_Z}+\left[A_{1pp}^X\right]c_{N_ZN_Z} \end{bmatrix},$$

$$[A_{uw}]=\begin{bmatrix} \left[APB_1^X\right]e_{11}+\left[ABP_1^X\right]f_{11} & \left[APB_1^X\right]e_{12}+\left[ABP_1^X\right]f_{12} & \dots & \left[APB_1^X\right]e_{1N_Z}+\left[ABP_1^X\right]f_{1N_Z} \\ \left[APB_1^X\right]e_{21}+\left[ABP_1^X\right]f_{21} & \left[APB_1^X\right]e_{22}+\left[ABP_1^X\right]f_{22} & \dots & \left[APB_1^X\right]e_{2N_Z}+\left[ABP_1^X\right]f_{2N_Z} \\ \dots & \dots & \dots & \dots \\ \left[APB_1^X\right]e_{N_Z1}+\left[ABP_1^X\right]f_{N_Z1} & \left[APB_1^X\right]e_{N_Z2}+\left[ABP_1^X\right]f_{N_Z2} & \dots & \left[APB_1^X\right]e_{N_ZN_Z}+\left[ABP_1^X\right]f_{N_ZN_Z} \end{bmatrix},$$

$$[A_{ww}]=\begin{bmatrix} \left[B_1^X\right]q_{11}+\left[B_{1pp}^X\right]d_{11} & \left[B_1^X\right]q_{12}+\left[B_{1pp}^X\right]d_{12} & \dots & \left[B_1^X\right]q_{1N_Z}+\left[B_{1pp}^X\right]d_{1N_Z} \\ \left[B_1^X\right]q_{21}+\left[B_{1pp}^X\right]d_{21} & \left[B_1^X\right]q_{22}+\left[B_{1pp}^X\right]d_{22} & \dots & \left[B_1^X\right]q_{2N_Z}+\left[B_{1pp}^X\right]d_{2N_Z} \\ \dots & \dots & \dots & \dots \\ \left[B_1^X\right]q_{N_Z1}+\left[B_{1pp}^X\right]d_{N_Z1} & \left[B_1^X\right]q_{N_Z2}+\left[B_{1pp}^X\right]d_{N_Z2} & \dots & \left[B_1^X\right]q_{N_ZN_Z}+\left[B_{1pp}^X\right]d_{N_ZN_Z} \end{bmatrix},$$

$$[A_{wu}]=[A_{uw}]^T,$$

$$[A_{mu}]=\begin{bmatrix} \left[A_1^X\right]m_{11} & \left[A_1^X\right]m_{12} & \dots & \left[A_1^X\right]m_{1N_Z} \\ \left[A_1^X\right]m_{21} & \left[A_1^X\right]m_{22} & \dots & \left[A_1^X\right]m_{2N_Z} \\ \dots & \dots & \dots & \dots \\ \left[A_1^X\right]m_{N_Z1} & \left[A_1^X\right]m_{N_Z2} & \dots & \left[A_1^X\right]m_{1N_Z} \end{bmatrix},$$

$$[A_{mw}]=\begin{bmatrix} \left[A_1^X\right]n_{11} & \left[A_1^X\right]n_{12} & \dots & \left[A_1^X\right]n_{1N_Z} \\ \left[A_1^X\right]n_{21} & \left[A_1^X\right]n_{22} & \dots & \left[A_1^X\right]n_{2N_Z} \\ \dots & \dots & \dots & \dots \\ \left[A_1^X\right]n_{N_Z1} & \left[A_1^X\right]n_{N_Z2} & \dots & \left[A_1^X\right]n_{1N_Z} \end{bmatrix}.$$

Here

$$g_{ij}=\int_{-H}^{H} G\left(2i-1\right)\left(2j-1\right)z^{2i+2j-4}dz, \qquad q_{ij}=\int_{-H}^{H} C_{zz}(2j-2)z^{2i+2j-4}dz,$$

$$c_{ij}=\int_{-H}^{H} C_{xx}z^{2i+2j-2}dz, \qquad d_{ij}=\int_{-H}^{H} Gz^{2i+2j-4}dz,$$

$$e_{ij}=\int_{-H}^{H} C_{xz}(2j-2)z^{2i+2j-4}dz, \qquad m_{ij}=\int_{-H}^{H} r\,z^{2i+2j-2}dz, \tag{A4}$$

$$f_{ij}=\int_{-H}^{H} G(2i-1)z^{2i+2j-4}dz, \qquad n_{ij}=\int_{-H}^{H} r\,z^{2i+2j-4}dz.$$

For two or more layers, the structure of the system matrix is

$$\left[A^{\Sigma}\right]=\begin{bmatrix} [A_{11}] & [A_{12}] & \dots & [A_{1N}] \\ [A_{21}] & [A_{22}] & \dots & [A_{2N}] \\ \dots & \dots & \dots & \dots \\ [A_{N1}] & [A_{N2}] & \dots & [A_{NN}] \end{bmatrix}. \tag{A5}$$

Here

$$[A_{11}]=[A],$$

and the matrixes $\left[A_{ij}\right]$ differ only by terms (A4). For example

$$[A_{12}]=\begin{bmatrix} [A_{uu}]_{12} & [A_{uw}]_{12} \\ [A_{wu}]_{12} & [A_{ww}]_{12} \end{bmatrix},$$

$$[A_{uu}]_{12}=\begin{bmatrix} \left[A_1^X\right]g^{12}{}_{11}+\left[A_{1pp}^X\right]c^{12}{}_{11} & \left[A_1^X\right]g^{12}{}_{12}+\left[A_{1pp}^X\right]c^{12}{}_{12} & \dots & \left[A_1^X\right]g^{12}{}_{1N_Z}+\left[A_{1pp}^X\right]c^{12}{}_{1N_Z} \\ \left[A_1^X\right]g^{12}{}_{21}+\left[A_{1pp}^X\right]c^{12}{}_{21} & \left[A_1^X\right]g^{12}{}_{22}+\left[A_{1pp}^X\right]c^{12}{}_{22} & \dots & \left[A_1^X\right]g^{12}{}_{2N_Z}+\left[A_{1pp}^X\right]c^{12}{}_{2N_Z} \\ \dots & \dots & \dots & \dots \\ \left[A_1^X\right]g^{12}{}_{N_Z1}+\left[A_{1pp}^X\right]c^{12}{}_{N_Z1} & \left[A_1^X\right]g^{12}{}_{N_Z2}+\left[A_{1pp}^X\right]c^{12}{}_{N_Z2} & \dots & \left[A_1^X\right]g^{12}{}_{N_ZN_Z}+\left[A_{1pp}^X\right]c^{12}{}_{N_ZN_Z} \end{bmatrix}. \tag{A6}$$

$$g^{12}{}_{ij}=2\int_{H}^{H_P} G\left(2i-1\right)\left(2j-1\right)z^{2i-2}\left(H+z\right)^{2j-2}dz, \quad c^{12}{}_{ij}=\int_{-H}^{H} C_{xx}z^{2i-1}\left(H+z\right)^{2j-1}dz. \tag{A7}$$

For the beam with the uniform layers all parameters g_{ij}, c_{ij}, e_{ij} may be found analytically for known integer.

Appendix B. The structure of system matrix for clamped-free beam

For example, in the case studied at the beginning of the paper ($f_k(x)=g_k(x)=\sin(kp\,x/2L)$), we obtain for the terms of the matrix $\left[A_1^X\right]$:

$$a(k,k)=L/2,\quad a(k,m)=\frac{L}{(|k-m|)}\sin\left(\frac{|k-m|p}{2}\right)-\frac{L}{(|k+m|)}\sin\left(\frac{|k+m|p}{2}\right), \tag{B1}$$

for the matrix $\left[A_{1P}^X\right]$

$$a_P(k,k)=\left(\sin\left(\frac{kp}{2}\right)\right)^2/2,\quad a_P(k,m)=\frac{k}{2}\left(\frac{1}{k+m}-\frac{1}{k-m}-\frac{\cos\left(\frac{(k+m)p}{2}\right)}{k+m}+\frac{\cos\left(\frac{(k-m)p}{2}\right)}{k-m}\right), \tag{B2}$$

for the matrix $\left[A_{1PP}^X\right]$

$$a_{PP}(k,k)=\left(\frac{kp}{2L}\right)^2\left(L-a(k,k)\right),\quad a_{PP}(k,m)=\frac{kp}{2L}\frac{km}{2L}\left(a(k,m)+2L\sin\left(\frac{(k+m)p}{2}\right)/(k+m)p\right). \tag{B3}$$

and for matrices $\left[A_1^X\right],\left[A_{1P}^X\right]\left[A_{1PP}^X\right],\left[AB_1^X\right],\left[APB_1^X\right],\left[ABP_1^X\right]$:

$$\begin{aligned} &b(i,j)=a(i,j),\quad b_P(i,j)=a_P(i,j),\quad b_{PP}(i,j)=a_{PP}(i,j),\\ &ab(i,j)=a(i,j),\quad ab_P(i,j)=a_P(i,j),\quad ba_P(i,j)=a_P(j,i). \end{aligned} \tag{B4}$$

The coefficient in Eq. (B4) also may be found analytically.

References

[1] D. Ross, E. E. Ungar, E. M. Kerwin. Damping of plate flexural vibrations by means of viscoelastic laminate. ASME. *Structural Damping.* 1959. pp. 49–88.

[2] E. M. Kerwin. Damping of flexural waves by a constrained viscoelastic layer. *Journal of the Acoustical Society of America.* 31 (7). 1959. pp. 952–962.

[3] R. A. DiTaranto. Theory of vibratory bending for elastic and viscoelastic layered finite length beams. *Transactions of the ASME. Journal of Applied Mechanics.* 32. 1965. pp. 881–886.

[4] D. J. Mead, S. Markus. The forced vibration of a three-layer, damped sandwich beam with arbitrary boundary conditions. *Journal of Sound and Vibration.* 10. 1969. pp. 163–175.

[5] J. M. Whitney, C. T. Sun, A higher order theory for extensional motion of laminated anisotropic shells and plates. *J. Sound Vib.* 30. 1973. pp. 85–97.

[6] R. B. Nelson, D. R. Lorch. A refined theory for laminated orthotropic plates. *ASME. J. Appl. Mech.* 41. 1974. pp. 177–183.

[7] J. N. Reddy. A simple higher-order theory for laminated composite plates. *ASME. J. Appl. Mech.* 51. 1984. pp. 745–752.

[8] K. P. Soldatos, T. Timarci. A unified formulation of laminated composite, shear deformable five-degree-of-freedom cylindrical shell theories. *Compos. Struct.* 25. 1993. pp. 165–171.

[9] T. Kant, K. Swaminathan. Estimation of transverse-interlaminar stresses in laminated composites – a selective review and survey of current developments. *Compos. Struct.* 49. 2000. pp. 65–75.

[10] N. J. Pagano. Exact solutions for composite laminates in cylindrical bending. *Journal of Composite Materials.* 3. 1969. pp. 398–411.

[11] S. Srinivas, C. V. Joga Rao, A. K. Rao. Flexural vibration of rectangular plates. *J. Appl. Mech.* 23. 1970. 430–436.

[12] A. K. Noor. Free vibration of multilayered composite plates. *AIAA J.* 11. 1973. pp. 1038–1039.

[13] K. Swaminathan, S. S. Patil. Analytical solutions using a higher order refined computational mode with

12 degrees of freedom for the free vibration analysis of antisymmetrical angle-ply plates. *Composite structures*. 82. 2008. pp. 209–216.

[14] K. H. Lo, R. M. Christensen. E. M. A. Wu. High-Order Theory of Plate Deformation. Part 2: Laminated Plates. *Journal of Applied Mechanics*. 44. Trans. *ASME, Series E*. 1977. pp. 669–676.

[15] B. M. Diveyev, M. M. Nykolyshyn. Refined numerical schemes for a stressed-strained state of structural joints of layered elements, *Journal of Mathematical Sciences*. 107. 2001. pp. 3666–3670.

[16] Z. Wu, W. Chen. Free vibration of laminated composite and sandwich plates using global-local higher-order theory. *Journal of Sound and Vibration*. 298. 2006. pp. 333–349.

[17] Reddy J. N. A review of refined theories of laminated composite plates. *Shock and Vibration Digest*. 22. 1990. pp. 3–17.

[18] E. Carrera. Historical review of zig-zag theories for multilayered plates and shells. *Appl. Mech. Rev*. 56. 2003. pp. 287–308.

[19] Hu Heng, Belouettar Salim, Potier-Ferry Michel, Daya El Mustafa. Review and assessment of various theories for modeling sandwich composites. *Compos. Struct*. 84. 2008. pp. 282–292.

[20] Z. Li, M. J. Crocker. A review of vibration damping in sandwich composite structures, *International Journal of Acoustics and Vibration*, 10. 2005. pp. 159–169.

[21] Carrera E., Demasi L. Multilayered finite plate element based on Reissner mixed variational theorem. Part II: numerical analysis. *Int. J. Numer. Methods Eng*. 55. 2002. pp. 253–296.

[22] L. Demasi. 13 hierarchy plate theories for thick and thin composite plates. *Compos. Struct*. 84. 2008. pp. 256–270.

[23] S. H. Zhang, H. L. Chen, X. P. Wang. Numerical parametric investigation of loss factor of laminated composites with interleaved viscoelastic layers. *Int. J. of Vehicle Noise and Vibration*. 2. 2006. pp. 62–74.

[24] A. L. Araujo, C. M. Mota Soares, J. Herskovits, P. Pedersen. Estimation of piezoelastic and viscoelastic properties in laminated structures. *Composite Structures*. 87. 2009. pp. 168–174.

[25] Jean-Marie Berthelot, Mustapha Assarar, Youssef Sefrani, Abderrahim El Mahi. Damping analysis of composite materials and structures. *Composite Structures*. 85. 2008. pp. 189–204.

[26] Yabin Liao, Valana Wells. Estimation of complex Young's modulus of non-stiff materials using a modified Oberst beam technique. *Journal of Sound and Vibration*. 316. 2008. pp. 87–100.

[27] K. DeBelder, R. Pintelon, C. Demol, P. Roose. Estimation of the equivalent complex modulus of laminated glass beams and its application to sound transmission loss prediction. *Mechanical Systems and Signal Processing*. 24. 2010. pp. 809–822.

[28] F. S. Barbosa, M. C. R. Farage. A finite element model for sandwich viscoelastic beams: Experimental and numerical assessment. Journal of Sound and Vibration. 317. 2008. pp. 91–111.

[29] Reddy J. N. On refined computational models of composite laminates. *Int. J. Numer. Meth. Eng*. 27. 1989. pp. 361–382.

[30] V. A. Matsagar, R. S. Jangid. Dynamic characterization of base-isolated structures using analytical shear-beam model. *International Journal of Acoustics and Vibration*. 11. 2006. pp. 132–136.

[31] L. Gelman, P. Jenkins, I. Petrunin, M. J. Crocker. Vibroacoustical damping diagnostics: complex frequency response function versus its magnitude. *International Journal of Acoustics and Vibration*. 11. 2006. pp. 120–124.

[32] Z. Li, M. J. Crocker. Effects of Thickness and Delamination on the Damping in Honeycomb-foam Sandwich Beams. *J. Sound. Vib*. 294. 2006. pp. 473–485.

[33] K. H. Hornig, G. T. Flowers. Performance of Heuristic Optimisation Methods in the Characterisation of the Dynamic Properties of Sandwich Composite Materials. *International Journal of Acoustics and Vibration*. 12. 2007. pp. 60–68.

[34] D. Backstrom, A.C. Nilsson. Modelling the vibration of sandwich beams using frequency-dependent parameters. *Journal of Sound and Vibration*. 300. 2007. pp. 589–611.

[35] T. S. Plagianakos, D. A. Saravanos. High-order layerwise mechanics and finite element for the damped dynamic characteristics of sandwich composite beams. *International Journal of Solids and Structures*. 41. 2004. pp. 6853–6871.

[36] B. Diveyev, I. Butiter, N. Shcherbina. Identifying the elastic moduli of composite plates by using high-order theories. Pt 1. Theoretical approach. *Mech. Compos. Mater*. Vol. 44, No. 1. 2008. pp. 25–36.

[37] B. Diveyev, I. Butiter, N. Shcherbina. Identifying the elastic moduli of composite plates by using high-order theories. Pt 2. Theoretical-experimental approach. *Mech. Compos. Mater*. Vol. 44, No. 2. 2008. pp. 139–144.

[38] B. Diveyev, I. Butiter, N. Shcherbina. Influence of fixation conditions and material anisotropy on the frequency spectrum of laminated beams. *Mech. Compos. Mater*. Vol. 47, No. 2. 2011. pp. 149–160.

[39] Bohdan Diveyev, Andrij Beshley, Solomiia Konyk, Ivan Kernytskyy. Identification of transverse elastic moduli of composite beams by using combined criteria. Materials of 22nd International Congress on Sound and Vibration. Vol. 2. 2015. Florence, Italy. (Electronic edition).

[40] Bohdan Diveyev. Identifying the elastic moduli of composite plates by using high-order theories. Ukrainian Journal of Mechanical Engineering and Material Science. Vol. 1, No. 1. pp. 63–82.